Simulating tracking detectors that rely on ionisation

brief history of simulation
principles of operation
simulation methods

Aerial photo of the LHC region

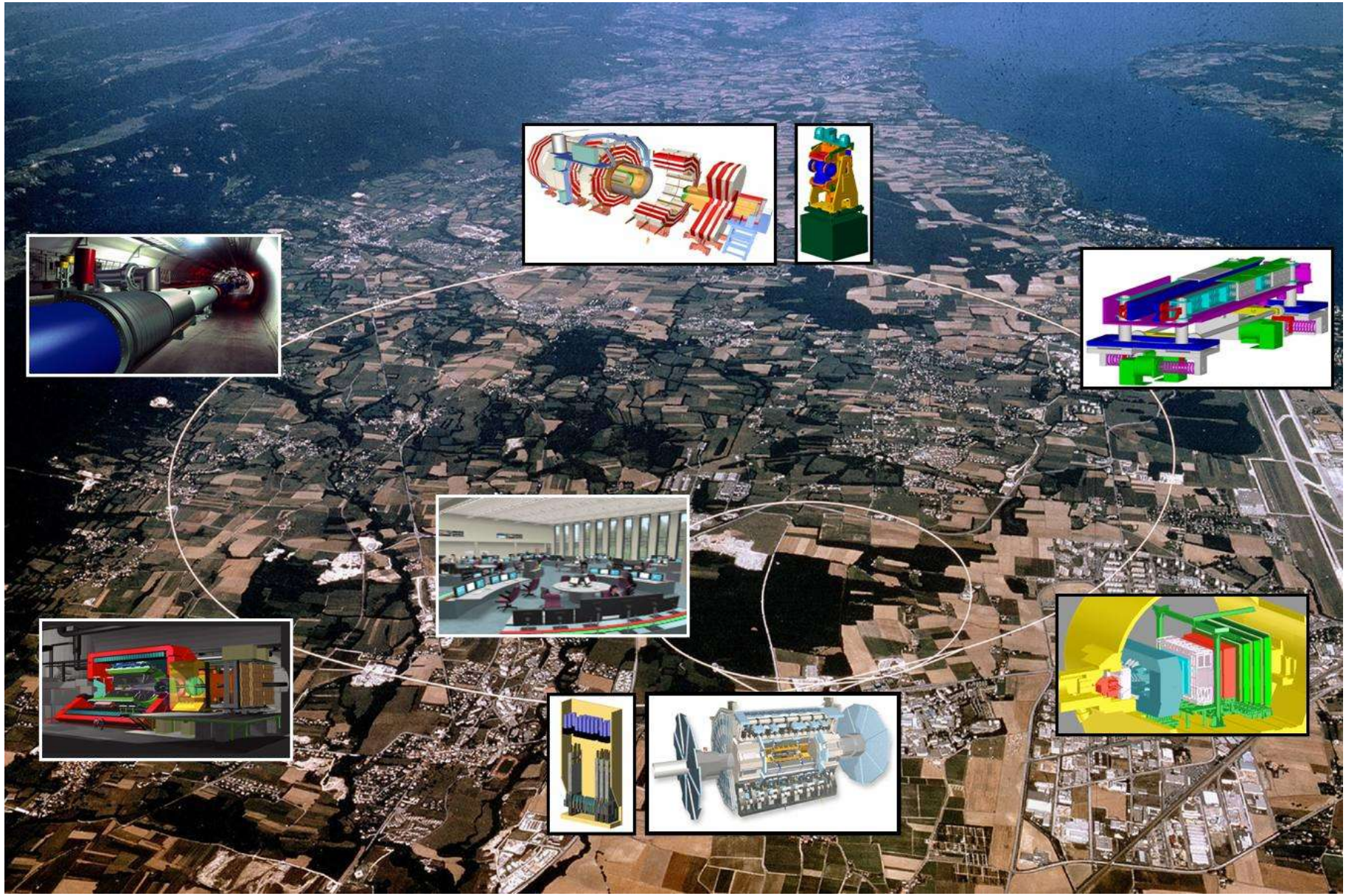

Alice

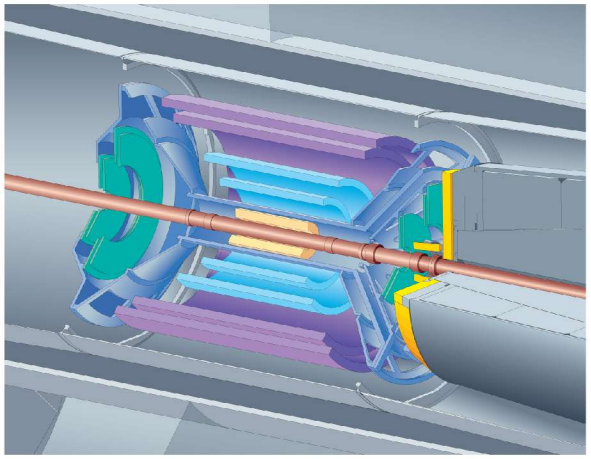

cosmic ray trigger

EM calorimetry

π/K/p identification

γ counter

0° energy

tracking

μ filter

e⁻ identification

time of flight

γ detection

magnet

μ system

0° energy

Example: history of $\mu^{\pm}$-tracking

- Why look for $\mu^{\pm}$?
  - major constituent of cosmic radiation in the atmosphere;
  - leptons are produced in early stages of the interactions;
  - leptons occur as decay products of sought-for particles;
  - penetrating, charged: easy to identify.
- Difficulties with $\mu^{\pm}$:
  - large background from $\pi^{\pm}$ decays.
- Some examples from history:
  - 1937: one of the discovery experiments;
  - 1989: an SPS fixed target experiment;
  - 2009: LHC experiments.

Cosmic radiation

- Outside the atmosphere, cosmic radiation consists of protons and light nuclei.
- On entering the atmosphere,
  - p+air $\rightarrow \pi^{\pm}, \pi^{0}$ (mostly)
  - $\pi^{\pm} \rightarrow \mu^{\pm}\nu$ ($c\tau$ ~ 7.8 m),
  - $\pi^{0} \rightarrow \gamma\gamma$ (prompt)
  - $\mu^{\pm} \rightarrow e^{\pm}\nu\nu$ ($c\tau$ ~ 660 m)
- We're irradiated by about 200 $\mu^{\pm}$/sec.m² !

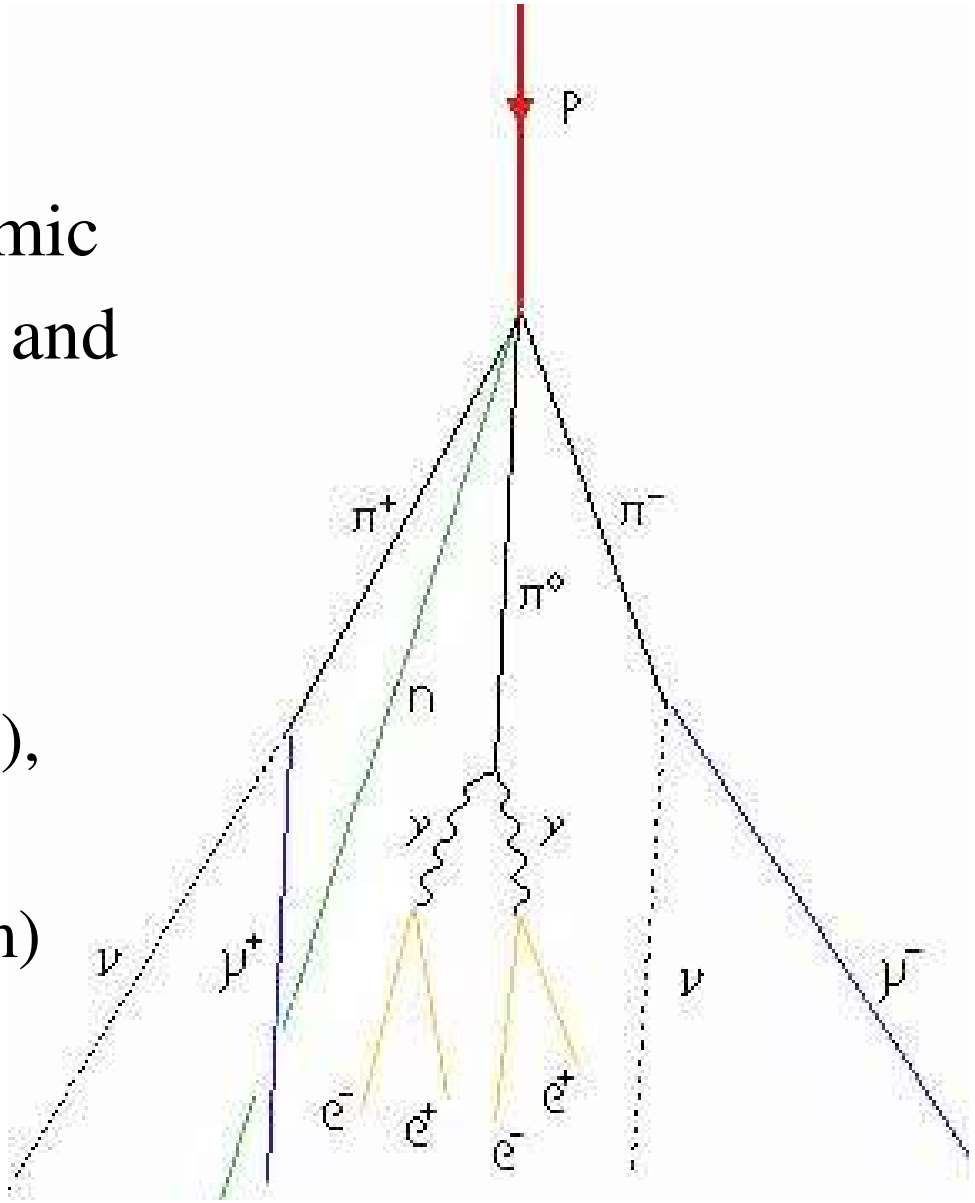

Geiger counter

- Detects radiation by discharge.
- Can count α and β particles (at low rates).
- No tracking capability.
- First models in 1908 by Hans Geiger, further developed from 1928 with Walther Müller.

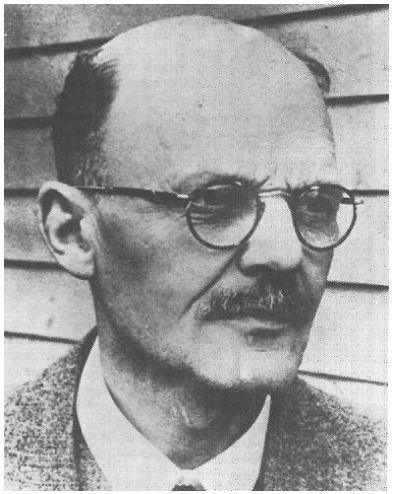

Hans Geiger
(1882-1945)

?

Walther Müller
(1905-1979)

A Geiger-Muller counter built in 1939 and used in the 1947-1950 for cosmic ray studies in balloons and on board B29 aircraft by Robert Millikan et al.

Made of copper, 30 cm long

Layout $\mu^{\pm}$ experiment 1937

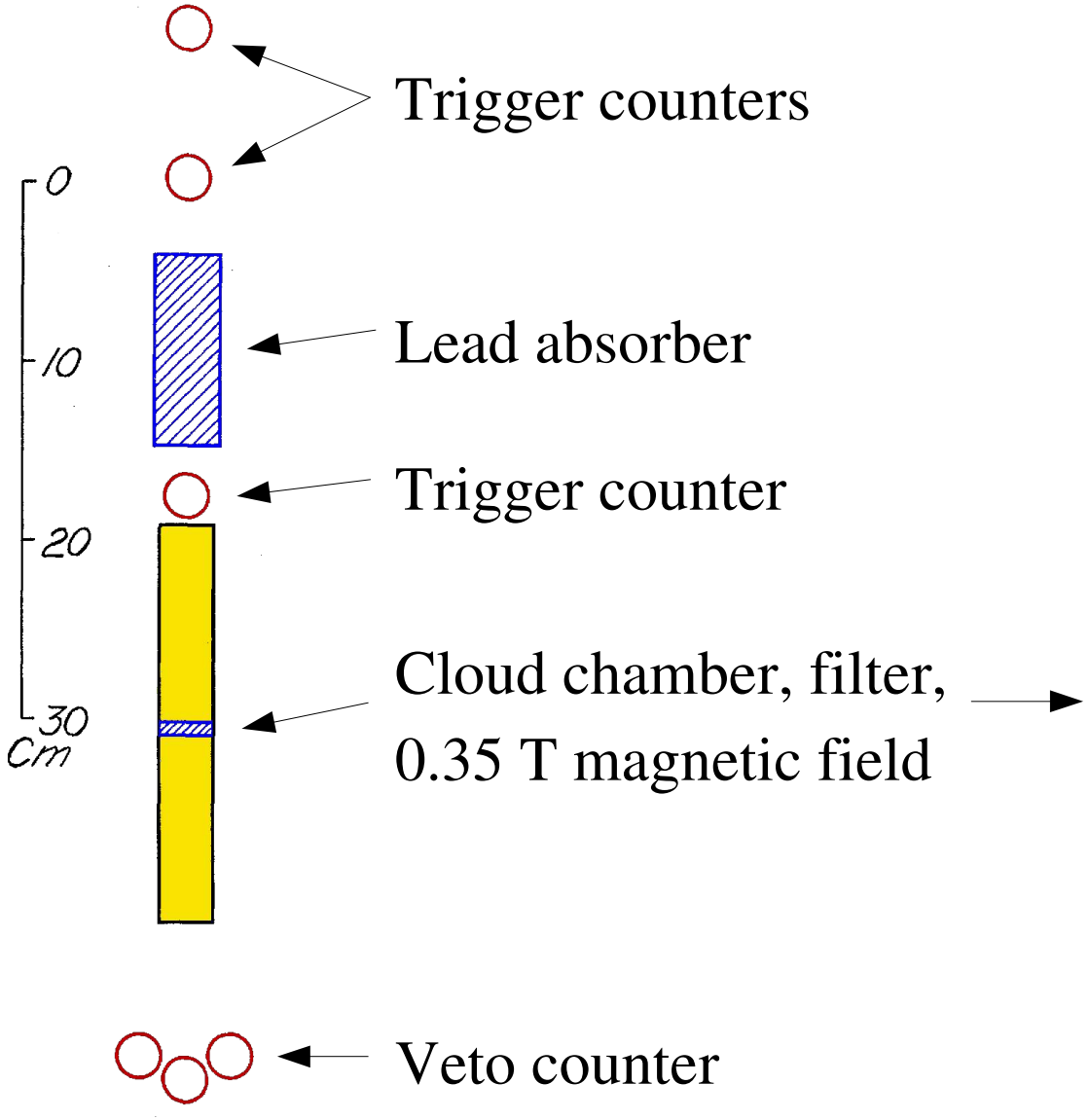

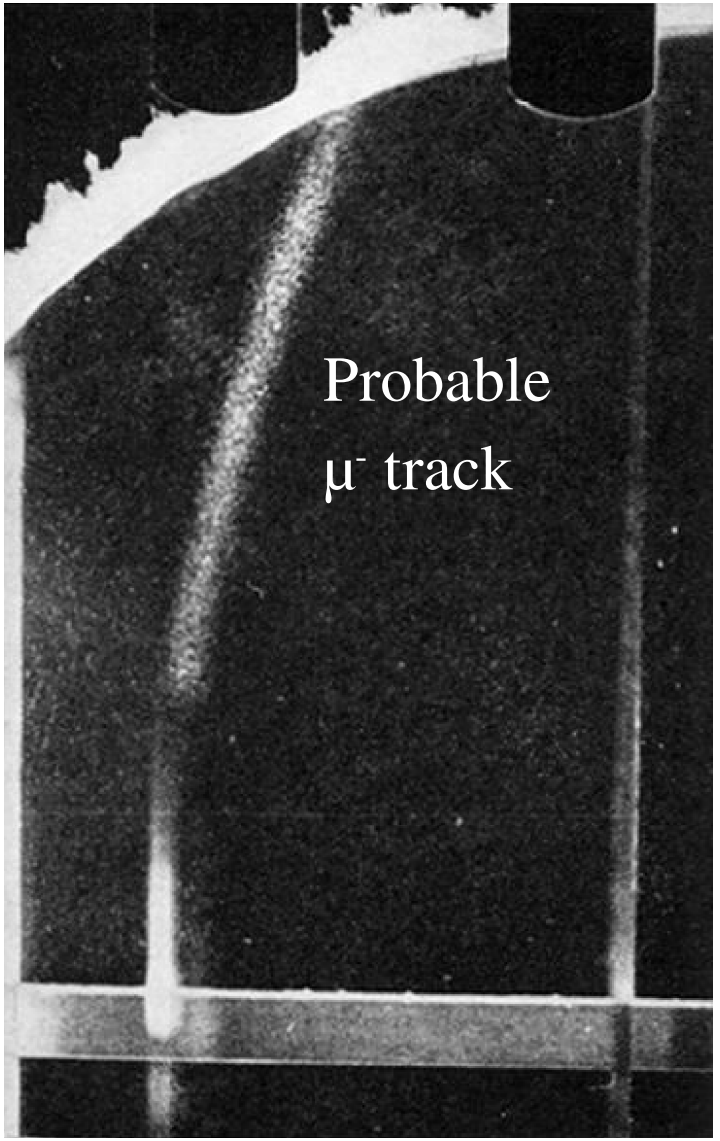

Track "B"

Findings $\mu^{\pm}$ experiment 1937

- Collected 4000 events, made 1000 photos, only 2 were singled out ... "A" is most likely a proton, but from the curvature of track "B" is a negatively charged particle.
- Ionisation density 6 $\times$ density of "usual thin tracks", *i.e.* high energy charged particles.
- Assuming ionisation $\propto 1/v^2$ + using the curvature, the estimated mass was 130 ± 25 % m_e or 66 ± 17 MeV (*cf.* PDG 2008 value: 105.658367 ± 0.000004 MeV).

- Ref: J. C. Street and E. C. Stevenson, Phys. Rev **52** (1937) 1003.

[Four Curies: Pierre, Marie, Irène and Pierre's father, around 1904 at the BIPM]

Simulation $\mu^{\pm}$ experiment 1937

- Electrically induced (!) gas discharge had been demonstrated as early as 1706 Francis Hauksbee (the Elder).
- Ionisation as a detection principle was recognised early:

> Becquerel discovered in 1896 the special radiating properties of uranium and its compounds. Uranium emits very weak rays which leave an impression on photographic plates. These rays pass through black paper and metals; they make air electrically conductive.
> [Pierre Curie, Nobel Lecture, June 6th 1905]

- Non-relativistic model of ionisation density was used (Bethe's relativistic formula dates back to 1932).
- These were not yet the days of detector simulation.

Helios/I (1989)

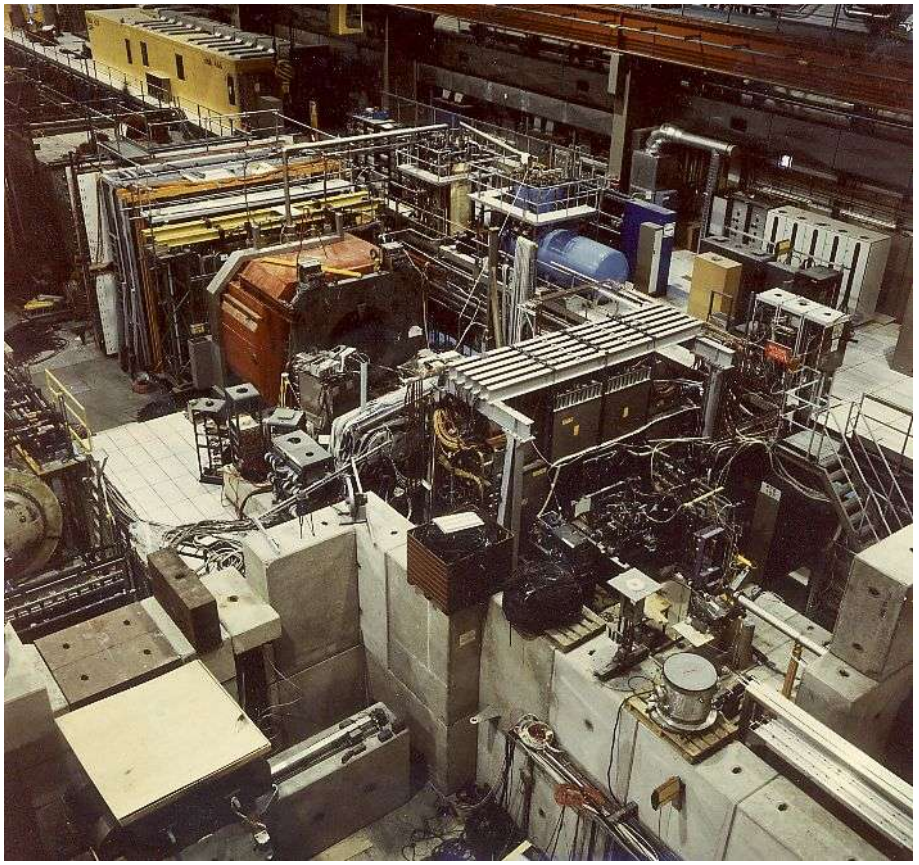

- The experiment recorded:
  - γ lAr calorimeter + crystals
  - $e^{\pm}$ lAr calorimeter + TRD
  - $\mu^{\pm}$ tracking chambers
  - ν nearly 4π calorimetry

- Data statistics:
  - 150 days with 10^6 p every 14 sec, $5\ 10^{11}$ p effective,
  - only 10^7 collisions recorded on tape.
  - of these, only of order 10^4 events were finally used.

Helios/I layout (1989)

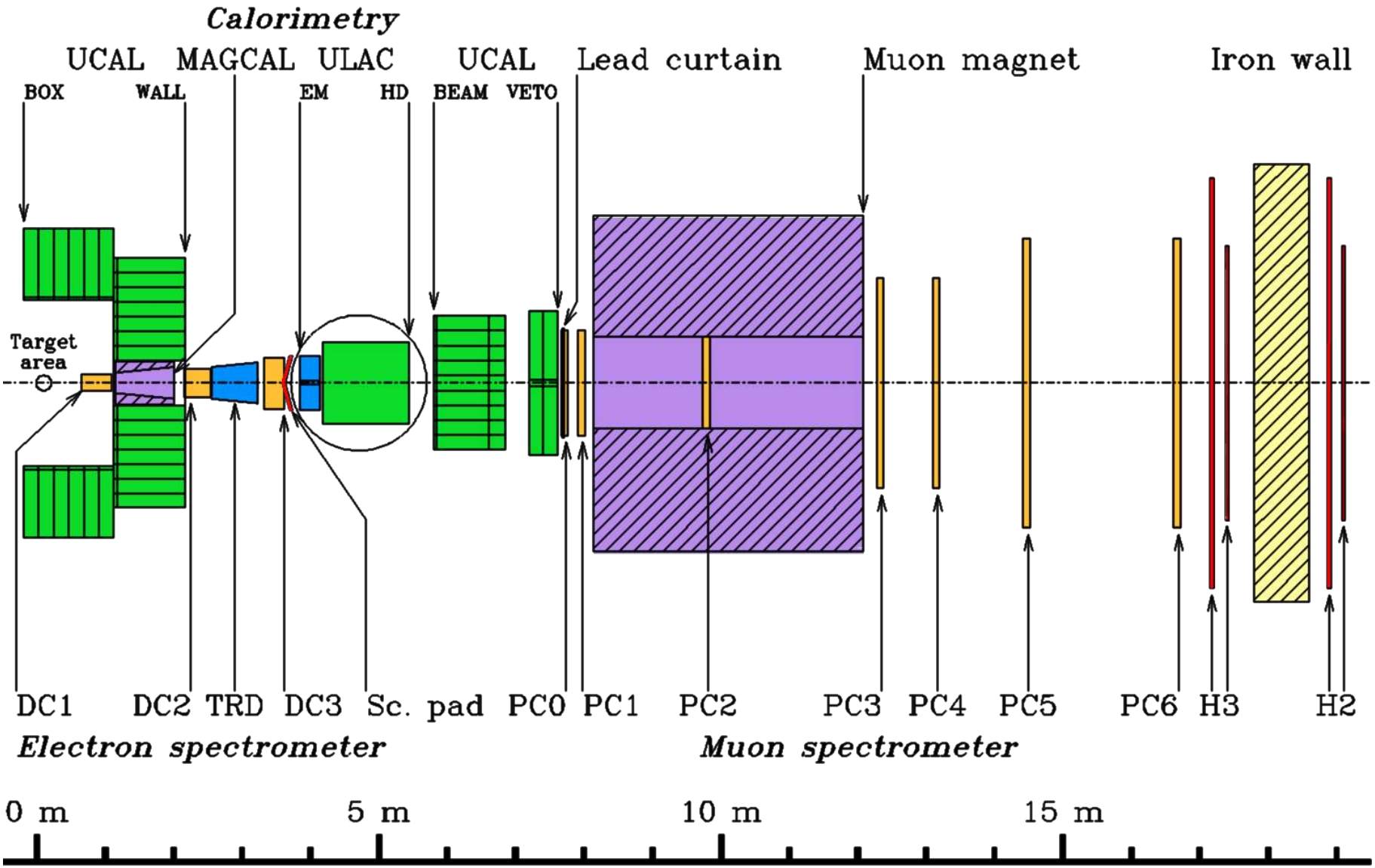

Helios/I tracking (1989)

- Three kinds of devices:
  - silicon strips near the vertex;
  - innovative drift chambers with CO_2 80 % Ar 20 %, 150-200 μm resolution;
  - large area multi-wire proportional chambers far downstream.

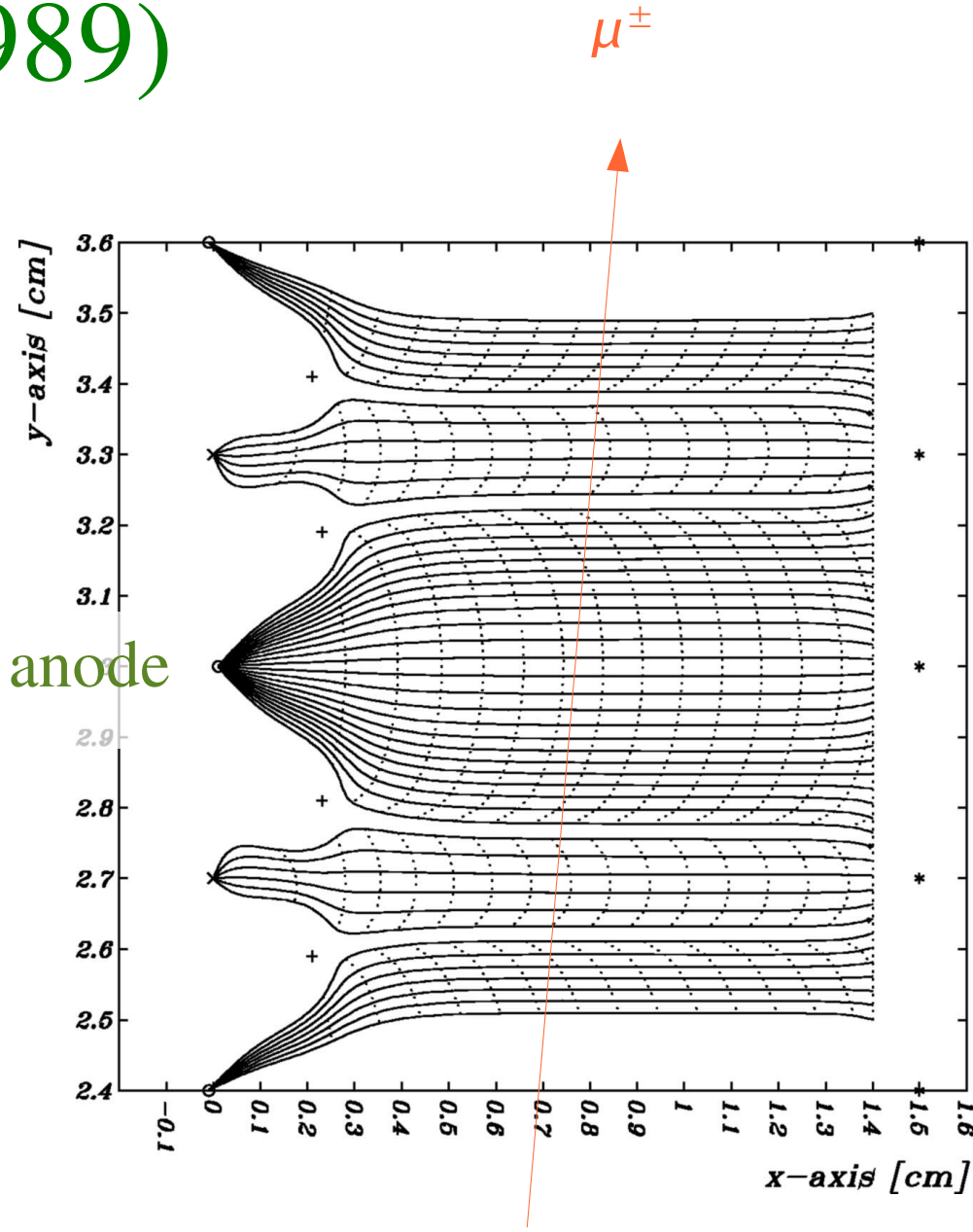

Helios/I $\mu^+\mu^-$ findings (1989)

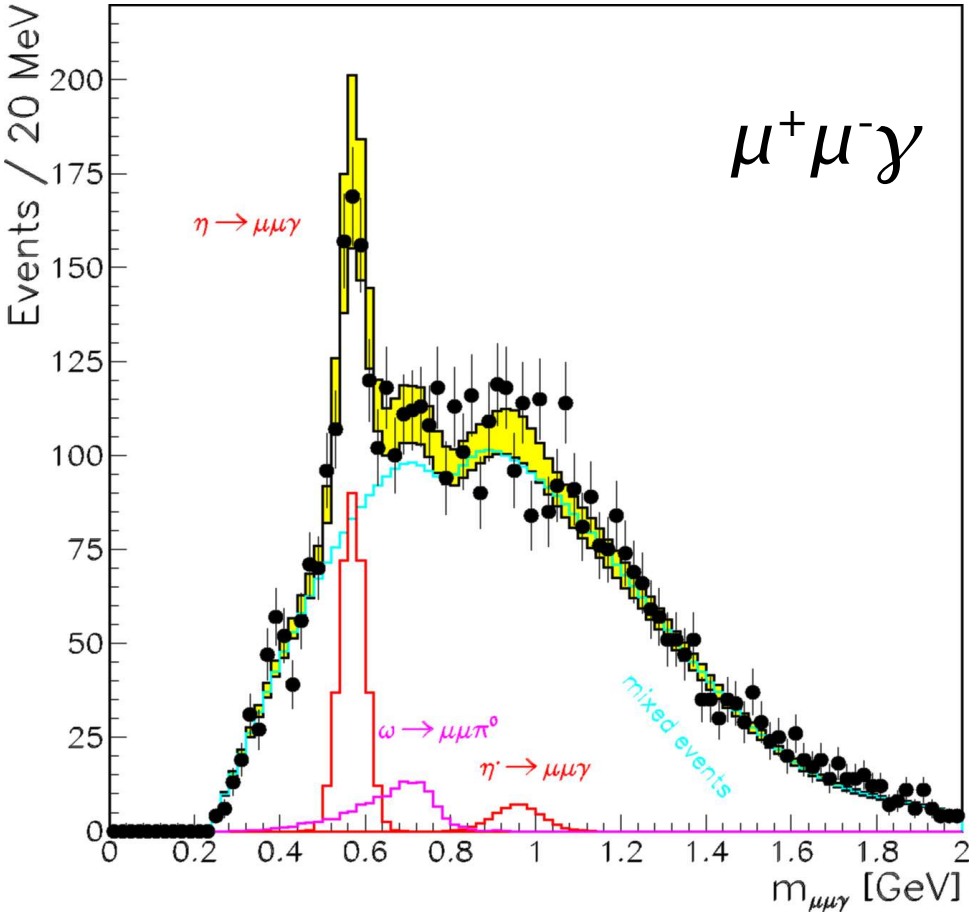

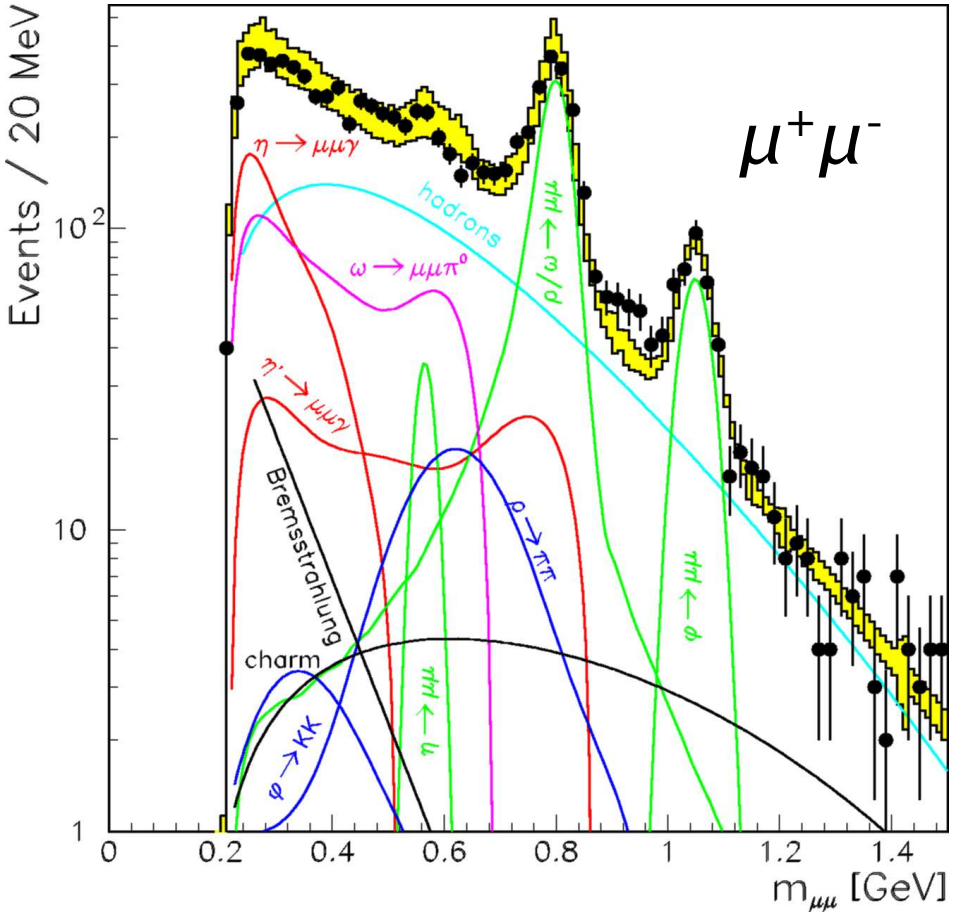

Simulation Helios/I (1989)

- Detector simulation was commonplace in 1989, Geant was widely used but didn't simulate gas-based devices.
- George Erskine had published from the 1970s a series of key papers on the electrostatics in gas-based detectors.
- The drift chambers had optimised drift patterns.
- Transport programs for gases had already been developed:
  - 1960: AV Phelps *et al.*, with LC Pitchford from 1982,
  - 1968: HR Skullerud
  - 1986: GW Fraser and E Mathieson
  - 1988: RE Robson and KF Ness,
  - 1989: Steve Biagi – the Magboltz programs.
- Still, the gas choice was based on practical experience, more than on calculations.

Atlas $\mu^{\pm}$ chambers (MDT)

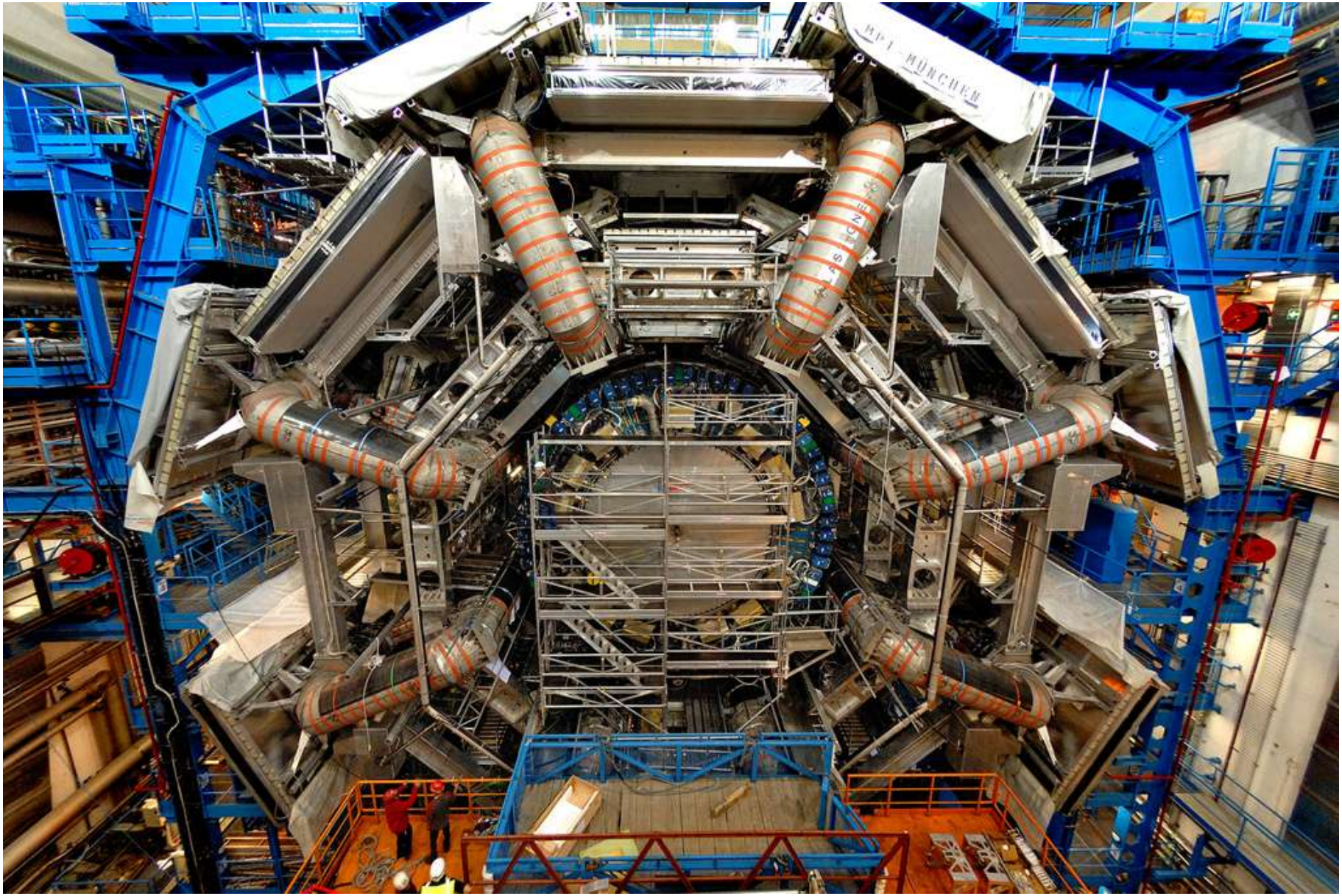

Atlas $\mu^{\pm}$ chambers (MDT)

Atlas MDT resolution

- Tube resolution is sensitive to:
  - details of ionisation patterns,
  - spatial extent δ-electrons,
  - e^- transport and diffusion,
  - gain and space charge,
  - resistor noise, t_p, filters ...
- Detector optimised combining test runs & detailed simulation.

- Reference: Werner Riegler, PhD thesis. Graphs for Ar 91 %, N_2 4 %, CH_4 5 % at 3 bar, which is not the mixture that will be used.

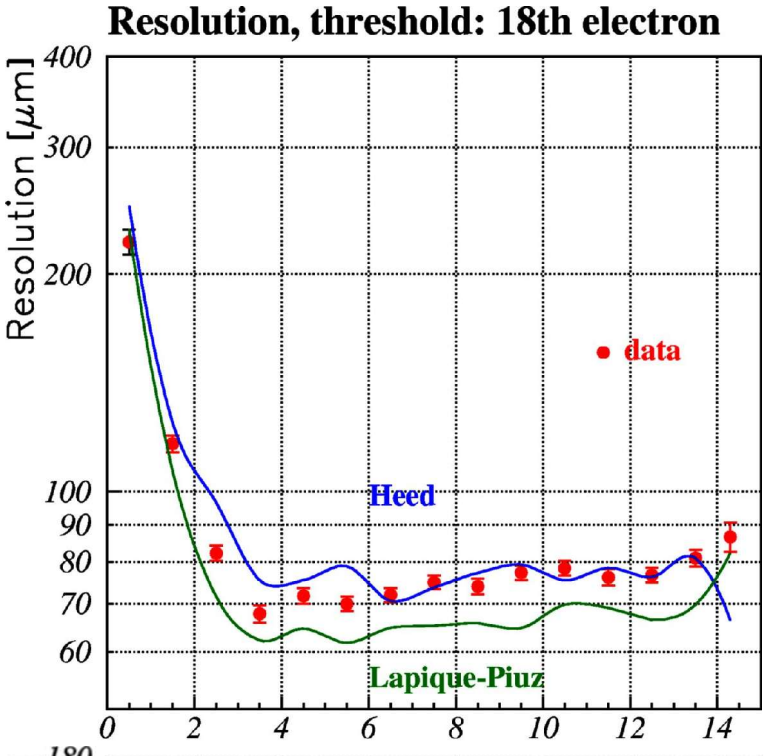

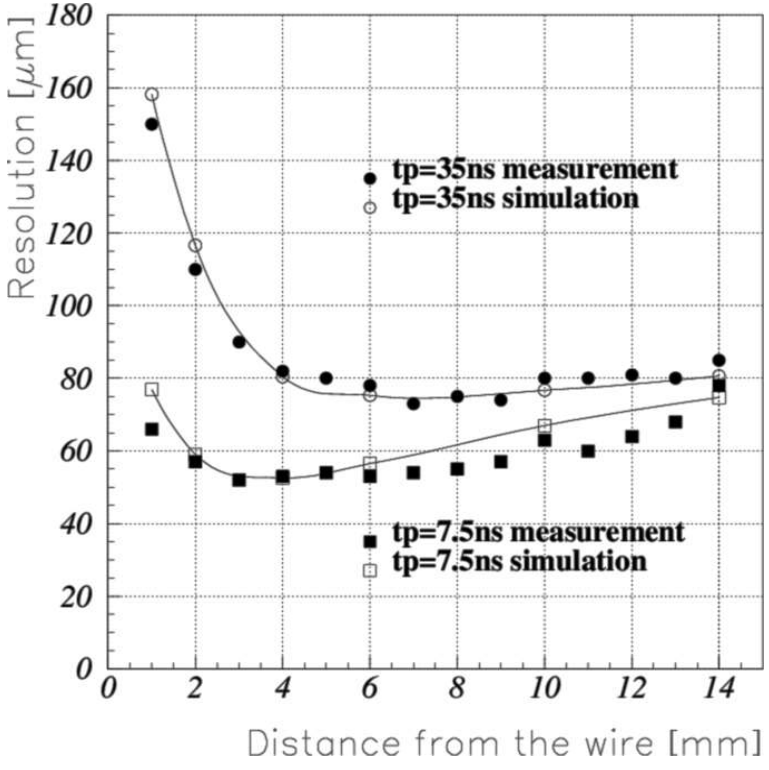

Micropattern devices: Micromegas

- Fast, rate tolerant tracking device
- 1994: Yannis Giomataris and Georges Charpak

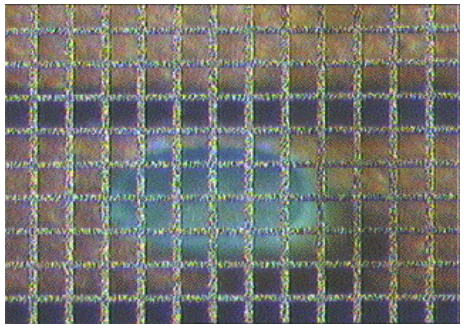

A mesh – holes of 30 μm

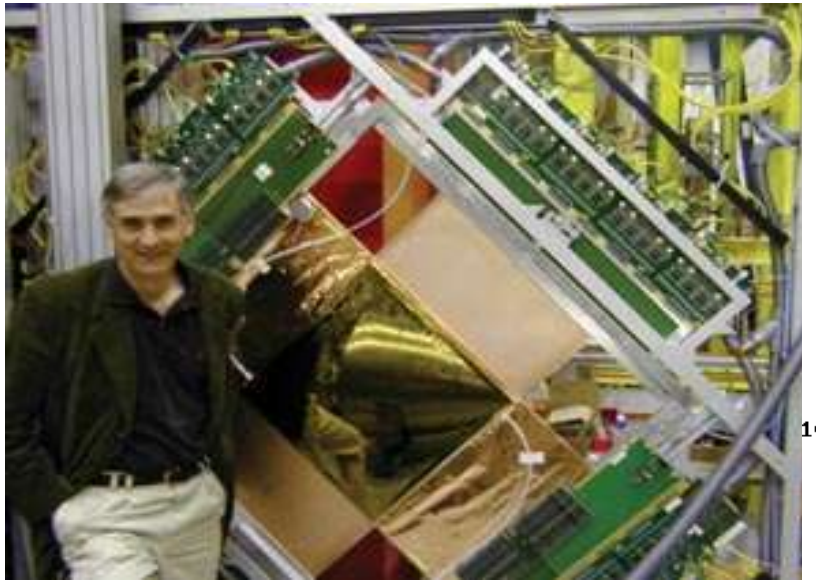

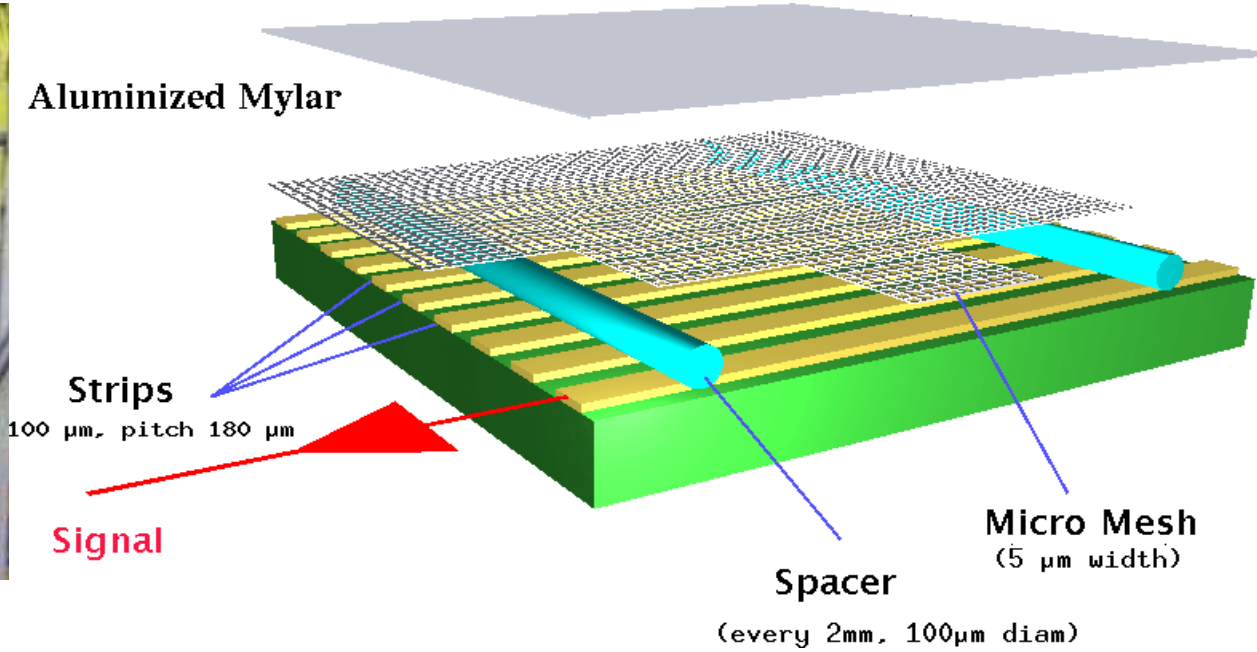

GEMs

- Acts as a “pre-amplifier”
- 1996: Fabio Sauli

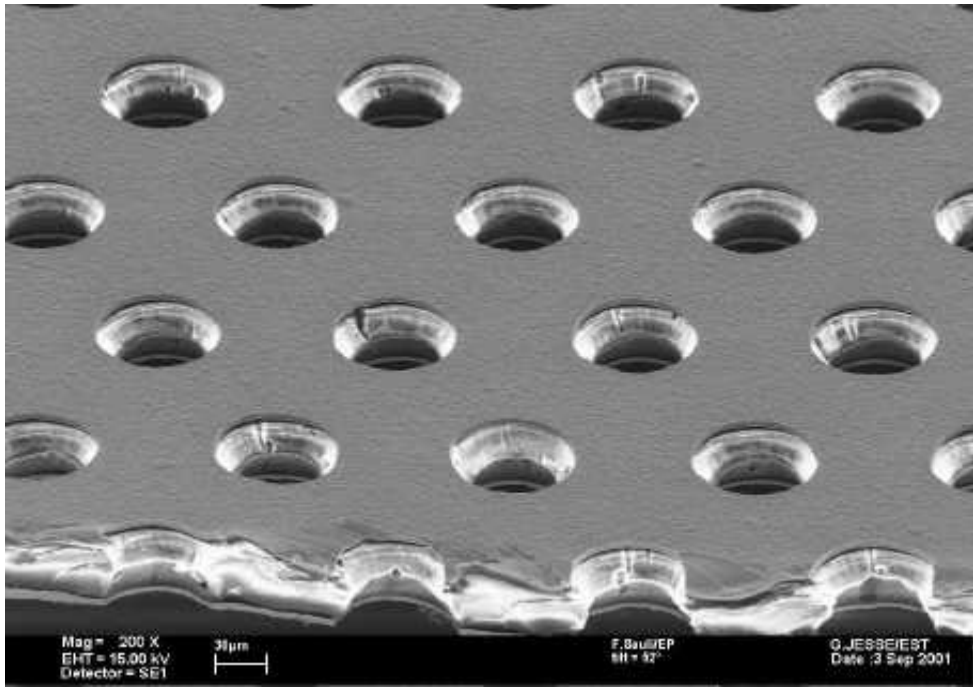

A few electrons enter here

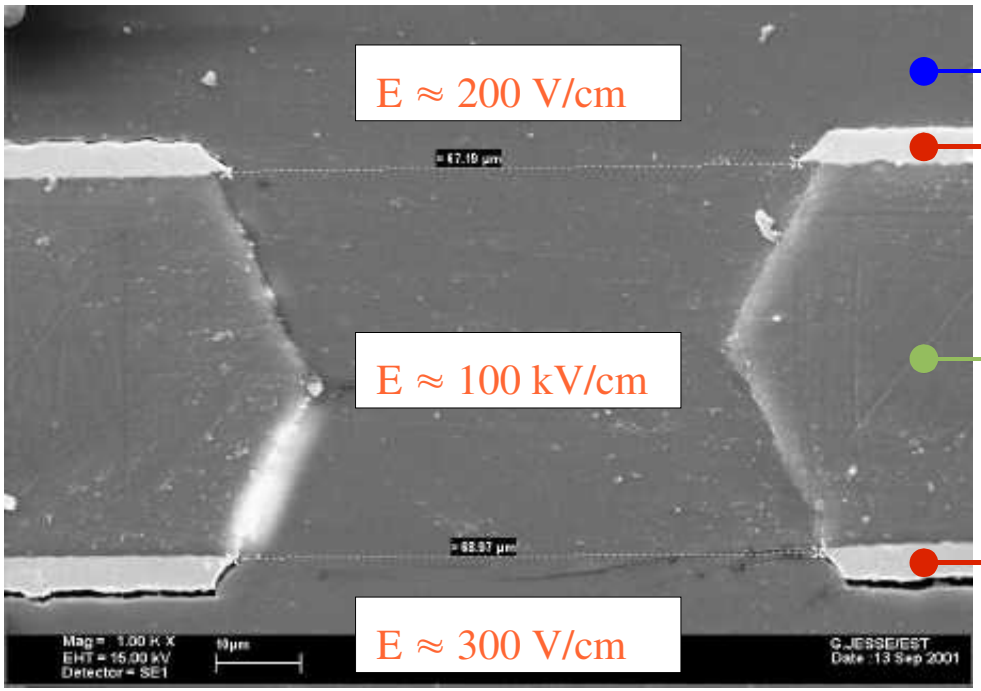

Gas

Metal

Dielectric

Metal

Fabio Sauli

Many electrons exit here

Simulation of micropattern devices

- Micropattern devices have characteristic dimensions that are comparable with the mean free path.

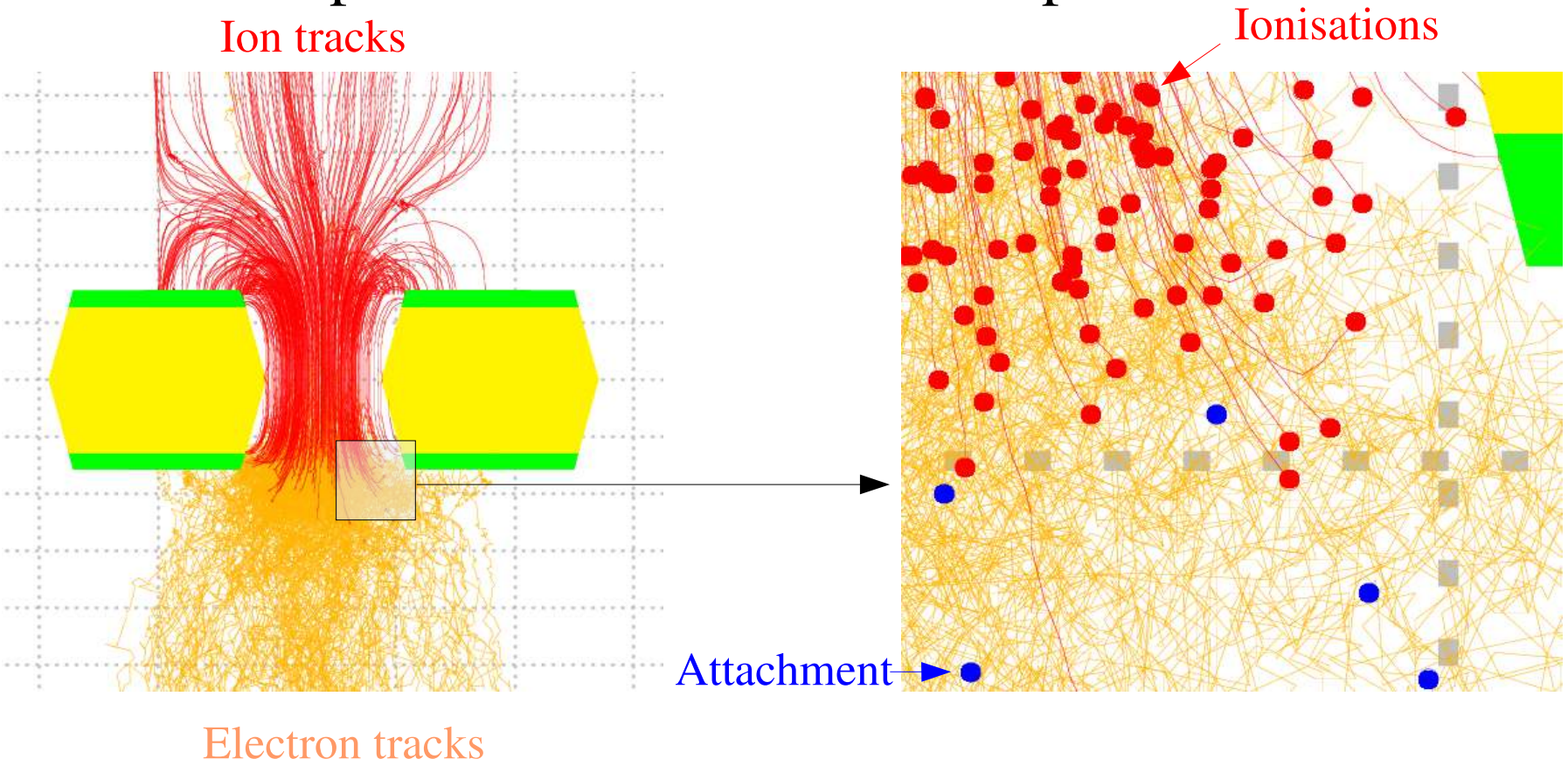

[Plot by Gabriele Croci and Matteo Alfonsi]

Trends in $\mu^{\pm}$ tracking

- Intrinsic resolution:
  - photographic detectors: 10-100 μm
  - MWPC: ~1 mm — detect wire hit
  - drift chambers: 150-250 μm — measure drift time
  - LHC experiments: 50-200 μm — gas, electronics ...
  - micropattern detectors: 20- 50 μm — small scale electrodes
  - semi-conductors: a few μm
- Relying on increasingly subtle sensitive medium properties.
- Better and better understanding of the operating principles is required to optimise the devices.

Principles of ionisation-based tracking

- These devices work according to similar principles:
  - a charged particle passing through the gas ionises some of the gas molecules;
  - the electric field in the gas volume transports the ionisation electrons and, in some areas, also provokes multiplication;
  - the charge movements (of electrons and ions) lead to induced currents in electrodes, and these currents are recorded.

Ionisation processes: Heed

Igor Smirnov

- PAI model or absorption of real photons:

  $Atom + \pi^- \rightarrow Ion^{+*} + \pi^- + e^-$

  $Atom + \gamma \rightarrow Ion^{+*} + e^-$ (photo-electric effect)

- Decay of excited states:

  $Ion^{+*} \rightarrow Ion^{++} + e^-$ (Auger)

  $Ion^{+*} \rightarrow Ion^{+} + \gamma$ (fluorescence)

  $Ion^{+*} \rightarrow Ion^{+*}$ (Coster-Kronig)

- Treatment of:
  - secondary photons, returning to the PAI model,
  - ionising photo-electrons and Auger-electrons, collectively known as δ-electrons:

  $e^- + Atom \rightarrow Ion^{+} + 2\, e^-$ (absorption of high-energy electrons)

Basic formulae of the PAI model

- Key ingredient: photo-absorption cross section $\sigma_\gamma(E)$

$$\frac{\beta^2\pi}{\alpha}\frac{\mathrm{d}\sigma}{\mathrm{d}E}=\frac{\sigma_\gamma(E)}{E}\log\left(\frac{1}{\sqrt{(1-\beta^2\epsilon_1)^2+\beta^4\epsilon_2^2}}\right)+$$ Relativistic rise

Cross section to transfer energy E

$$\frac{1}{N\bar{h}c}\left(\beta^2-\frac{\epsilon_1}{|\epsilon|^2}\right)\theta+$$ Čerenkov radiation

$$\frac{\sigma_\gamma(E)}{E}\log\left(\frac{2m_e c^2\beta^2}{E}\right)+$$ Resonance region

$$\frac{1}{E^2}\int_0^E\sigma_\gamma(E_1)\,\mathrm{d}E_1$$ Rutherford scattering

With: $\epsilon_2(E)=\frac{N_e\bar{h}c}{EZ}\sigma_\gamma(E)$

$$\epsilon_1(E)=1+\frac{2}{\pi}\mathrm{P}\int_0^\infty\frac{x\,\epsilon_2(x)}{x^2-E^2}\mathrm{d}x$$

$$\theta=\arg(1-\epsilon_1\beta^2+i\,\epsilon_2\beta^2)=\frac{\pi}{2}-\arctan\frac{1-\epsilon_1\beta^2}{\epsilon_2\beta^2}$$

Photo-absorption in argon

- Argon has 3 shells, hence 3 groups of lines:

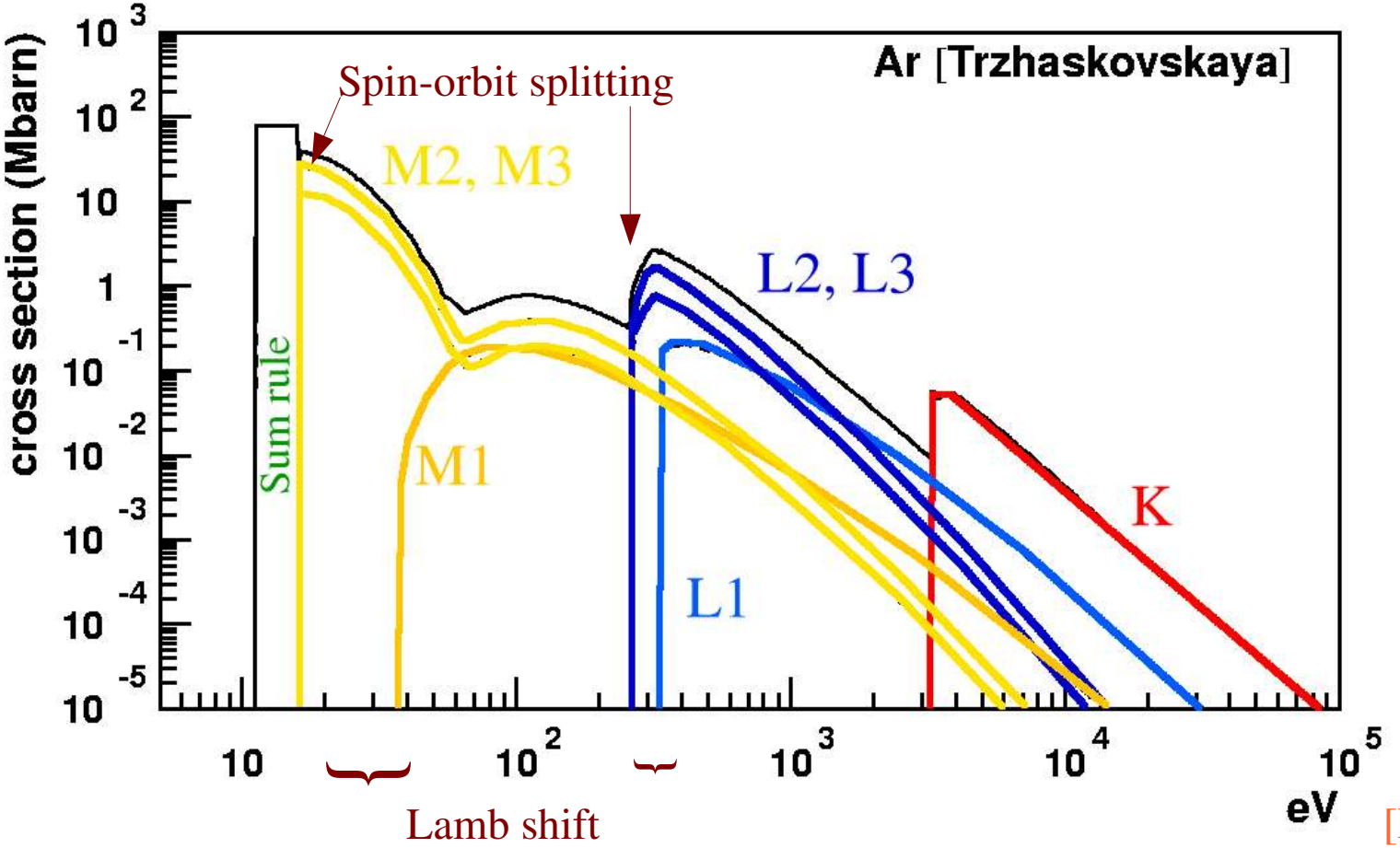

K = 1s

L1 = 2s
L2 = 2p 1/2
L3 = 2p 3/2

M1 = 3s
M2 = 3p 1/2
M3 = 3p 3/2

[Plot from Igor Smirnov]

Importance of the PAI model terms

- All electron orbitals (shells) participate:
  - outer shells: frequent interactions, few electrons;
  - inner shells: few interactions, many electrons.
- All terms in the formula are important.

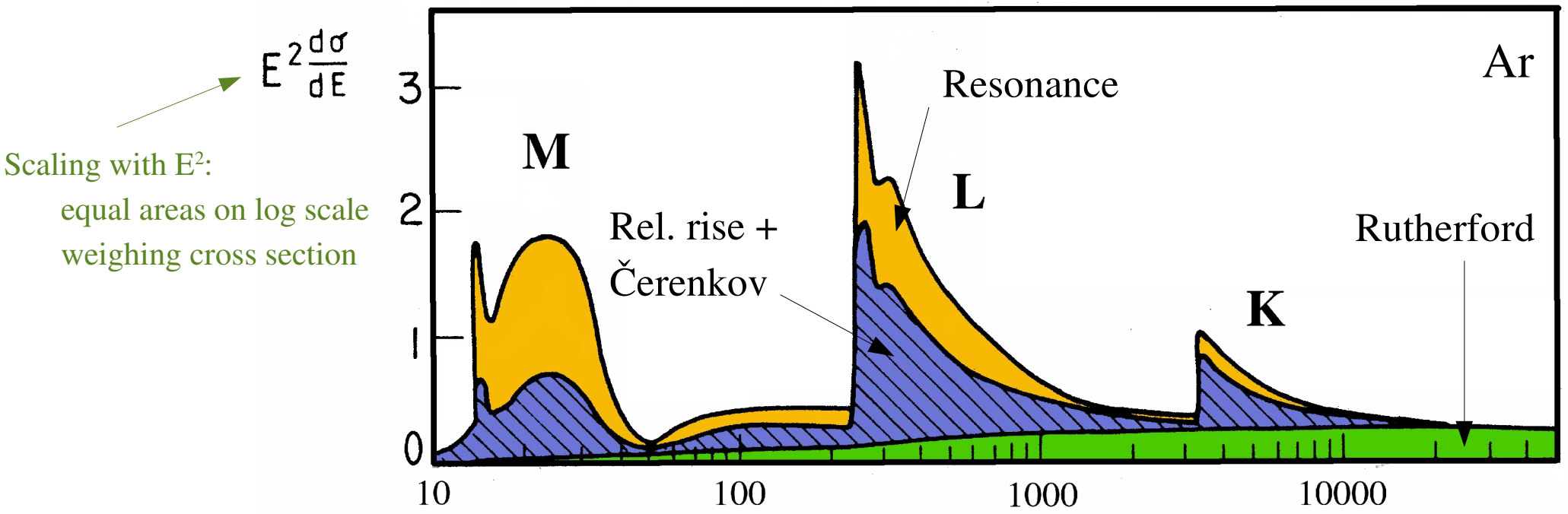

[Adapted from Allison & Cobb, Ann. Rev. Nucl. Part. Sci. **30** (1980) 253-298]

How well is the cross section known ?

- Agreement is not impressive at the shell edges !

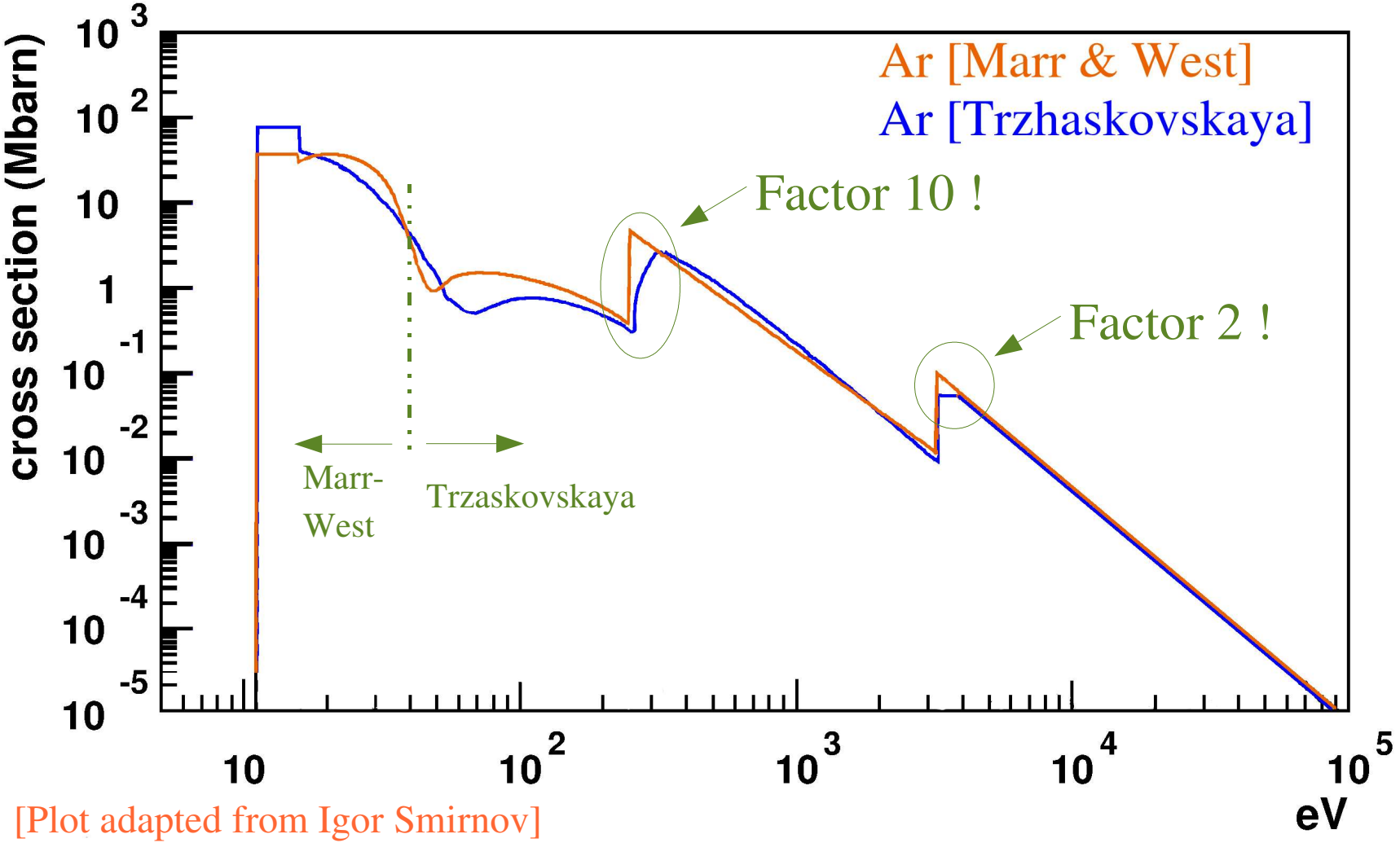

[Plot adapted from Igor Smirnov]

Energy Loss (PAI Model)

optical loss function Im(-1/$\epsilon(E)$) of solid Si

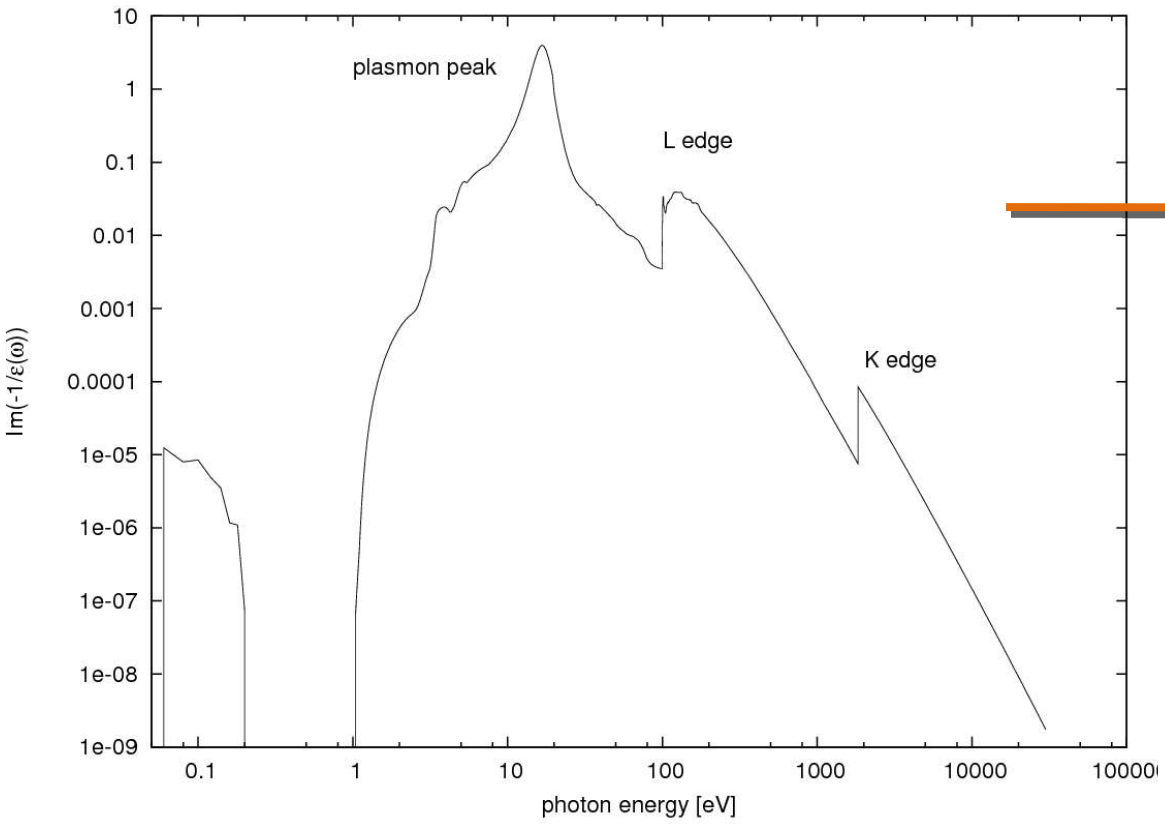

differential cross-section

$$\frac{\mathrm{d}\sigma}{\mathrm{d}E} = \left(\frac{z^2\alpha_f}{\beta^2\pi N_{\mathrm{el}}\hbar c}\right)\mathrm{Im}\frac{-1}{\epsilon(E)}\log\frac{2m\beta^2c^2}{E|1-\beta^2\epsilon(E)|} +$$

$$\left(\frac{z^2\alpha_f}{\beta^2\pi N_{\mathrm{el}}\hbar c}\right)\left(\beta^2 - \frac{\epsilon'(E)}{|\epsilon(E)|^2}\right)\left(\frac{\pi}{2} - \arctan\frac{1-\beta^2\epsilon'(E)}{\beta^2\epsilon''(E)}\right) +$$

$$\left(\frac{z^2\alpha_f}{\beta^2\pi N_{\mathrm{el}}\hbar c}\right)\frac{1}{E^2}\int_0^{\epsilon} E'\,\mathrm{Im}\frac{-1}{\epsilon(E')}\,\mathrm{d}E'$$

$$\left(\sigma(E) \rightarrow \mathrm{Im}\frac{-1}{\epsilon(E)}\right)$$

loss spectrum (5 GeV/c π, 20.5 μm Si)

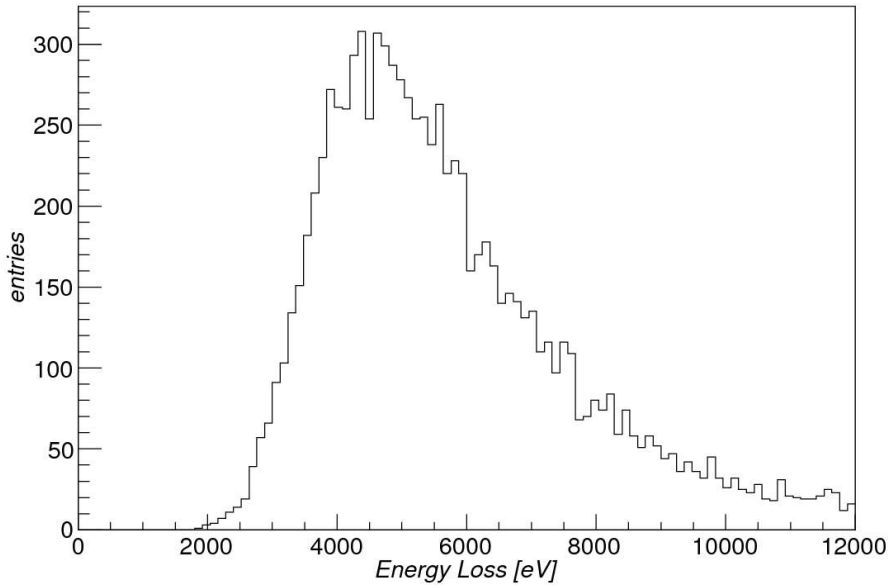

Primary Ionization: calculate number of e/h pairs from $W = 3.6$ eV, $F \approx 0.12$ or perform detailed simulation of secondary electron cascade

Field calculation techniques

- Analytic calculations:
  - almost all 2d structures made of wires, planes !
  - fast and precise, if applicable.
- Finite elements:
  - 2d and 3d structures, with or without dielectrics;
  - several major intrinsic shortcomings.
- Integral equations or Boundary element methods:
  - equally comprehensive without the intrinsic flaws;
  - wrought with difficulties, not yet widely available.
- Finite differences:
  - still used for iterative, time-dependent calculations.

Analytic field calculations

- Analytic calculations rely on complex functions because of two remarkable properties:
  - Cauchy-Riemann equations:
    - The real part of *any* complex analytic function is a valid potential function.
  - Conformal mapping:
    - Almost *every* analytic geometric transformation of a valid potential, is a valid potential too.
- Applicability:
  - a surprisingly large class of detectors can be calculated with this technique: drift chambers, TPCs, MWPCs, hexagonal counters – but only in 2d.

Cauchy-Riemann equations

Augustin Louis Cauchy
(Aug 21st 1789 – May 23rd 1857)

- Express the existence of a derivative of a complex analytic function $f = u + \mathrm{i}\, v$

$$f'(z) = \frac{\partial f}{\partial x} = \frac{\partial u}{\partial x} + \mathrm{i}\frac{\partial v}{\partial x} \qquad \frac{\partial u}{\partial x} = \frac{\partial v}{\partial y}$$

$$= \frac{\partial f}{\partial \mathrm{i}\, y} = -\mathrm{i}\frac{\partial u}{\partial y} + \frac{\partial v}{\partial y} \qquad \frac{\partial v}{\partial x} = -\frac{\partial u}{\partial y}$$

Georg Friedrich Bernhard Riemann
(Sep 17st 1826 – Jul 20th 1866)

- Imply that u is harmonic:

$$\frac{\partial^2 u}{\partial x^2} = \frac{\partial^2 v}{\partial x \partial y} = \frac{\partial^2 v}{\partial y \partial x} = \frac{-\partial^2 u}{\partial y \partial y} \qquad \frac{\partial^2 u}{\partial x^2} + \frac{\partial^2 u}{\partial y^2} = 0$$

Jean le Rond d'Alembert
(Nov 16th 1717 –Oct 29th 1783)

- Reference: A.L. Cauchy, *Sur les intégrales définies* (1814). This *mémoire* was read in 1814, but only submitted to the printer in 1825.

Conformal mappings

- A geometric transformation through *any* analytic function maps any valid potential function to another, equally valid, potential function.

- Applications:
  - Cartesian to polar coordinates;
  - off-axis wire inside a tube;
  - external and internal areas of polygones;
  - ...

Conformal mappings - examples

- Schwarz-Christoffel transformation of a half-plane to the external part of a rectangle:

$$z \to \int_0^z \frac{\mathrm{d}\xi}{\sqrt{\xi(\xi-1)(\xi-a)}} = \frac{2}{\sqrt{a}} \mathrm{sn}^{-1}\left(\sqrt{z}, \frac{1}{\sqrt{a}}\right)$$

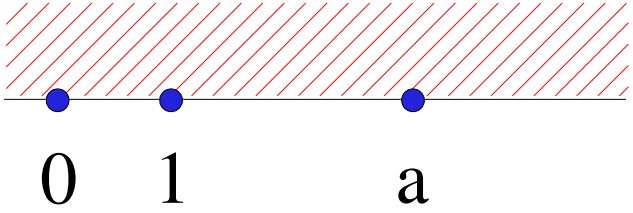

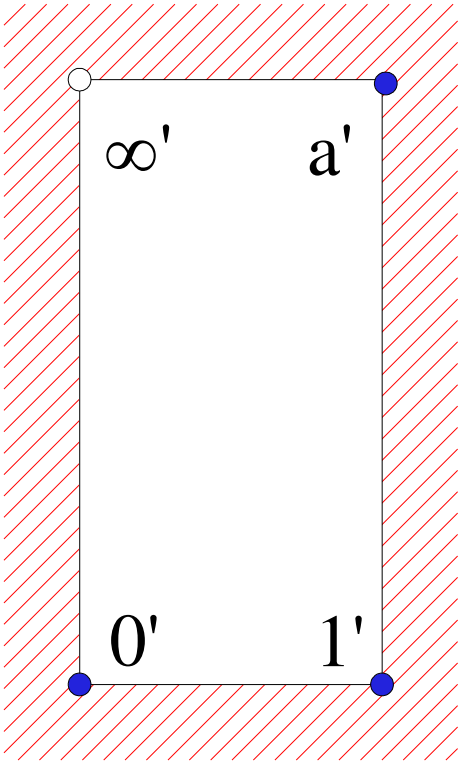

Why not 3d ?

Caspar Wessel (1745-1818)
Jean-Robert Argand (1768-1822)
Johann Carl Friedrich Gauss (1777-1855)
Sir William Rowan Hamilton (1805-1865)
Charles Sanders Peirce (1839-1914)
Georg Frobenius (1849-1917)

- The complex numbers $(\mathbb{R}^2,+,\times)$ form a field, like the real numbers $(\mathbb{R},+,\times)$, but $(\mathbb{R}^3,+,\times)$ does not. As a result, 2d arithmetic can be done with complex numbers, but there is no 3d equivalent for this.

- It can be proven that only $\mathbb{R}$ and $\mathbb{C}$ can form a commutative division algebra (field).

- $(\mathbb{R}^4,+,\times)$ can be made into a non-commutative division algebra known as quaternions, but this would not be help since $\nabla \cdot E$ links all dimensions.

Finite elements – common applications

- The finite element method is widely used to tackle a class of 2d *and* 3d differential equations:
  - heat flow: $\nabla^2 T = 1/k \ \partial T/\partial t$ (T: temperature)
  - stress analysis: $\nabla \cdot \sigma + F = 0$ (σ: stress tensor)
  - magnetic fields: $\nabla \times B = \mu J$ (J: current)
  - electric fields: $\nabla \cdot E = \rho/\epsilon$ (ρ: charge)
- All equations are already written (heat) or can be written in harmonic form: $\nabla^2 V = q$
  - V and q are scalar for heat and electric fields, vectorial for stress and magnetic fields.
  - Time-dependent problems are computed in steps.

Terminology

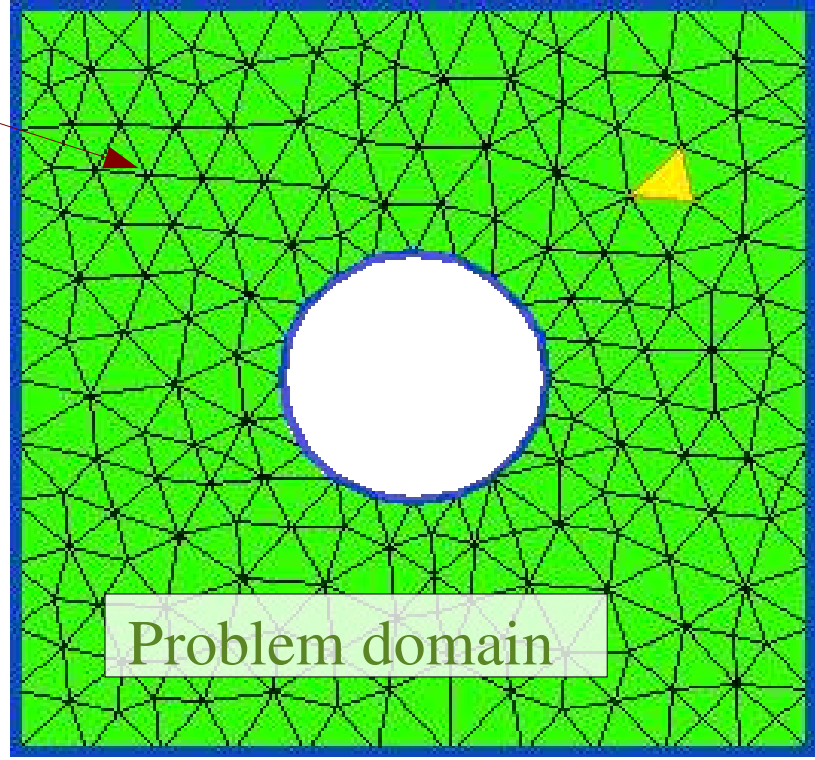

- A *mesh* subdivides the *problem domain* into *elements*.
- *Elements* are simple geometric shapes: triangles, squares, tetrahedra, hexahedra etc.
- Important points of *elements* are called *nodes*. It is usual that several *elements* have a *node* at one and the same location.

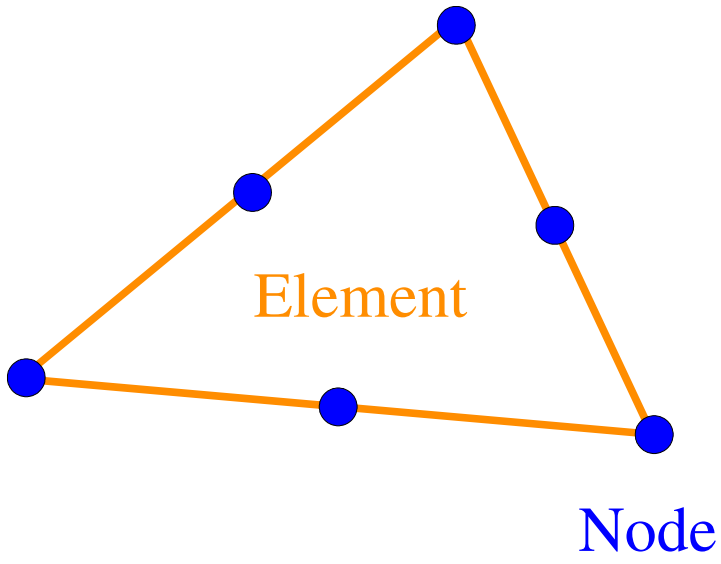

Shape functions - interpolation

- Each node has its own *shape function* $N_i(r)$:
  - continuous functions (usually polynomial),
  - defined only throughout the body of the element,
  - $N_i(r) = 1$ when $r = r_i$ i.e. on node i,
  - $N_i(r) = 0$ when $r = r_j$, $i \neq j$ i.e. on all other nodes.

- The solution of a finite element problem is given in the form of potential values at each of the nodes of each of the elements: v_i.

- At interior points of an element: $V(r) = \sum v_i N_i(r)$

Shape functions: 2nd order triangle

- The 2nd order triangle and tetrahedron are widely used. The triangle shape functions are:
  - $N_1 = \xi_1(2\,\xi_1 - 1)$
  - $N_2 = \xi_2(2\,\xi_2 - 1)$
  - $N_3 = \xi_3(2\,\xi_3 - 1)$
  - $N_4 = 4\,\xi_2\xi_3$
  - $N_5 = 4\,\xi_1\xi_3$
  - $N_6 = 4\,\xi_1\xi_2$
- The shape functions for tetrahedra are analogous.
- These elements too are isoparametric.
- Depending on the location of the mid-point nodes, the edges can be parabolically curved. This feature is used by e.g. Ansys but not by Maxwell.

Are polynomial N_i suitable for V ?

- Polynomial shape functions imply a polynomial potential, here a 3.2 cm tube + 30 μm wire at 3 kV:

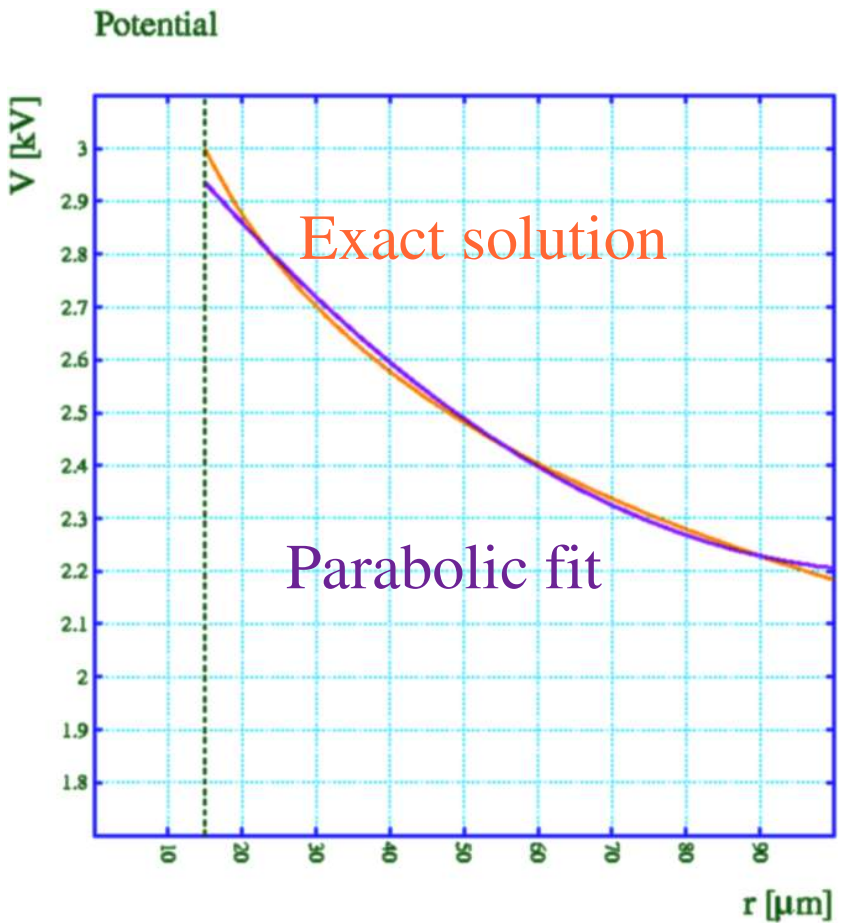

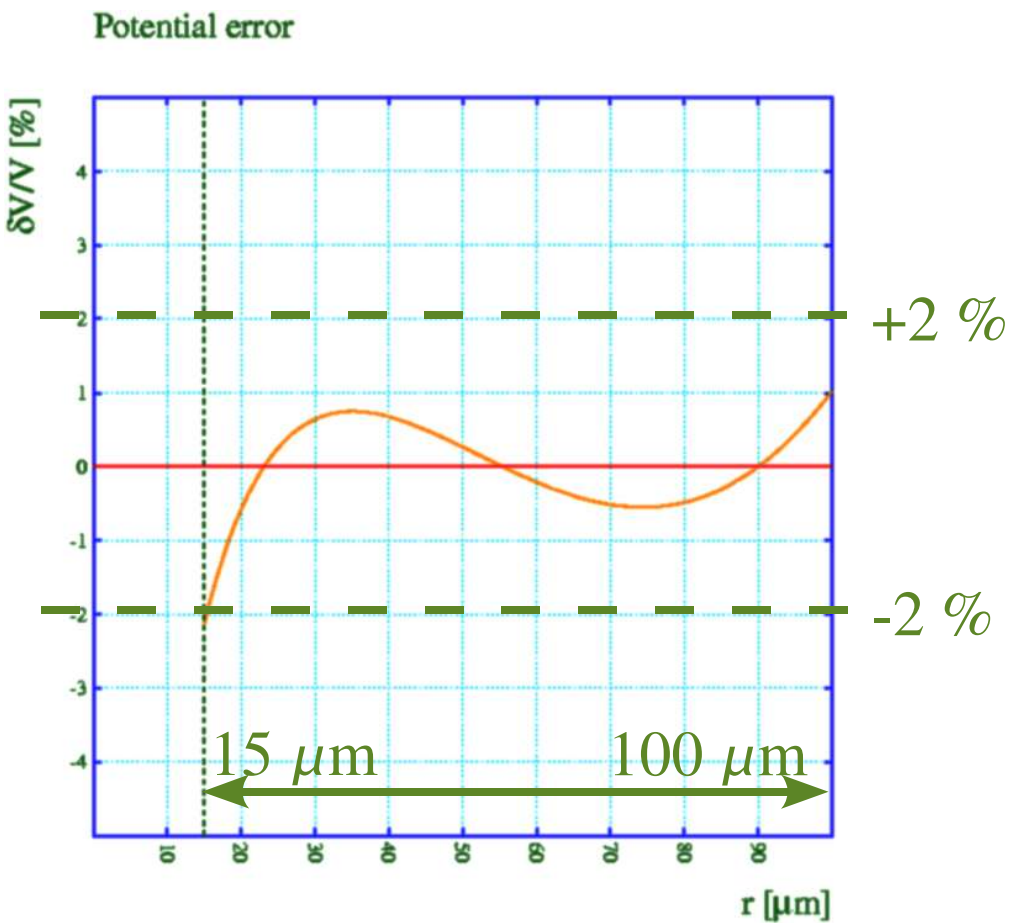

Are polynomial N_i suitable for E ?

- ... and a polynomial E field that is one order lower !

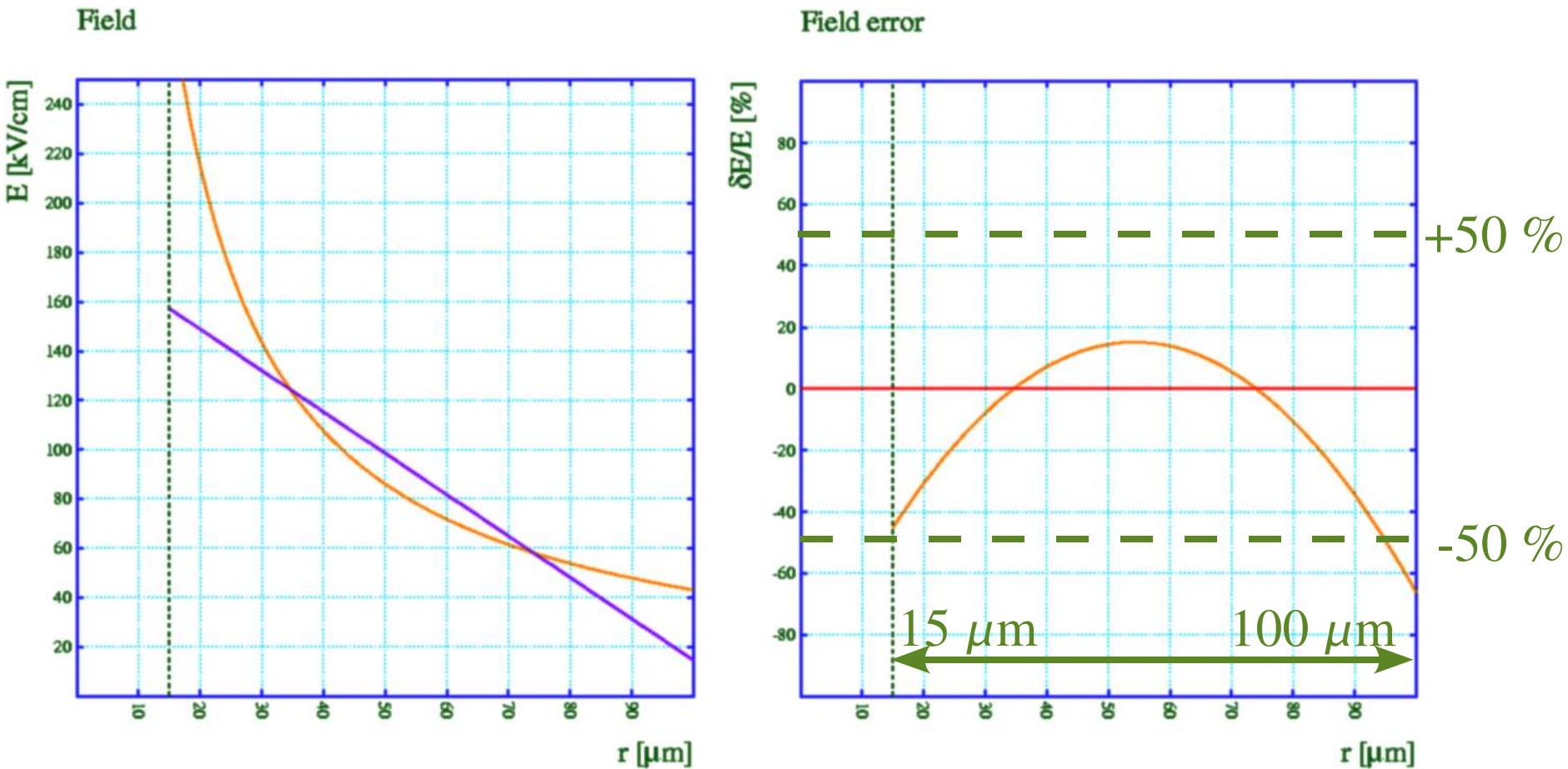

Continuity across boundaries

- Across element boundaries, the potential is guaranteed to be continuous.

- Example for a 2nd order triangle:
  - each edge shared by 2 elements, has 3 nodes;
  - the finite element method computes a unique potential for each node, i.e. the potential at the node is the same seen from both elements;
  - the potential is parabolic in each element, therefore also along each line in each element, and 3 points fully constrain a parabola.

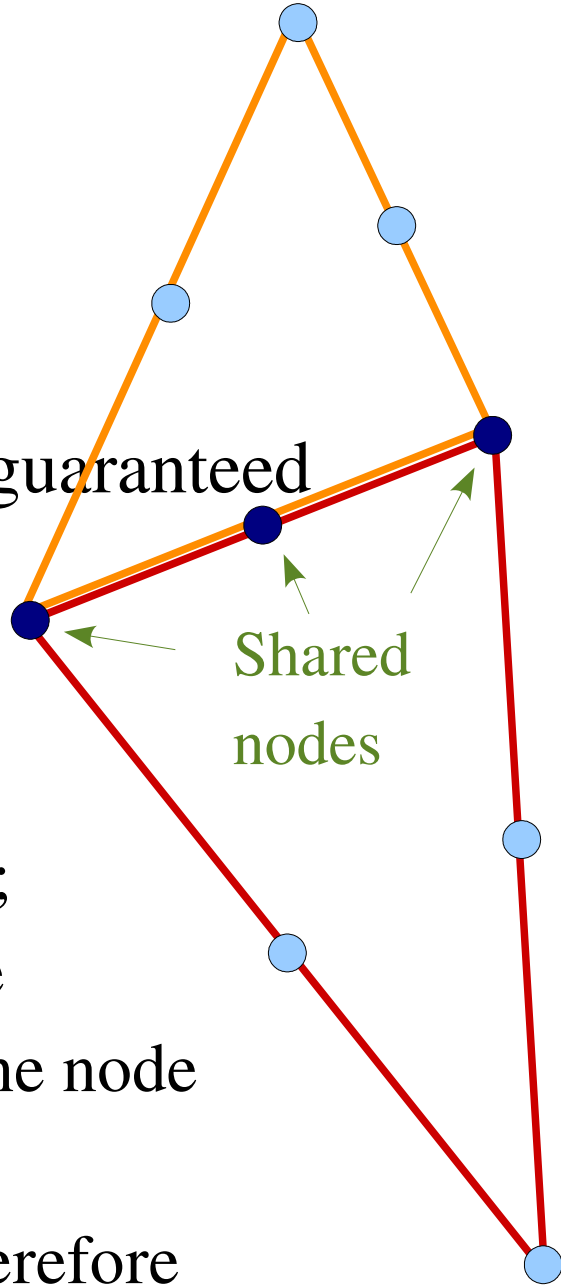

Continuity: the *E* field

- But ... the components of the *E* field look like the roofs of Nice: locally linear, and discontinuous.

Photo from: http://www.06nice.com/somvol/fotaer/gfoaer.htm

The price to pay for finite elements

- Finite element programs focus on the wrong thing:
  - they solve V well, but we do not really need it:
    - Quadratic shape functions can do a fair job at approximating $V \approx \log(r)$ potentials.
    - Potentials are continuous.
  - E is what we use, but:
    - Gradients of quadratic shape functions are linear and are not suited to approximate $E \approx 1/r$, left alone $E \approx 1/r^2$.
    - Electric fields are discontinuous at element boundaries.
    - A local accuracy of ~50 % in high-field areas is normal.
- In exchange, we get a lot of flexibility.

Food for thought ...

- “The Finite Element Method is a very useful tool which can make a good engineer better, but it can make a bad engineer dangerous.”
  [Robert D. Cook, Professor of Mechanical Engineering University of Wisconsin, Madison]

- One wonders what the Finite Element Method can do in the hands of a physicist.

Drift Field

Poisson equation

$$\nabla \cdot (\epsilon E) = \frac{\rho}{\epsilon_0}$$

electrons, acceptors

$$\rho = e(p - n + N_D - N_A) + \rho_t$$

holes, donors, traps, fixed charges

iterative calculation of drift field

Continuity equation (drift-diffusion model)

$$j_n = n \mu_n E - D_n \nabla n \qquad j_p = -p \mu_p E - D_p \nabla p$$

$$\frac{\partial n}{\partial t} = -\nabla \cdot j_n + G_n - R_n \qquad \frac{\partial p}{\partial t} = -\nabla \cdot j_p + G_p - R_p$$

TCAD

Synopsys TCAD (http://www.synopsys.com/Tools/TCAD/Pages/default.aspx): part of Sentaurus process and device simulation package

Create device structure (materials and contacts) and define doping concentrations → meshing → apply boundary conditions, select physical models to be used (e.g. mobility, impurities, charge deposition→ iterative numerical solution of Poisson equation + continuity equations for given boundary conditions
provides an extensive set of physical models → very valuable as reference

Example: silicon strip detector

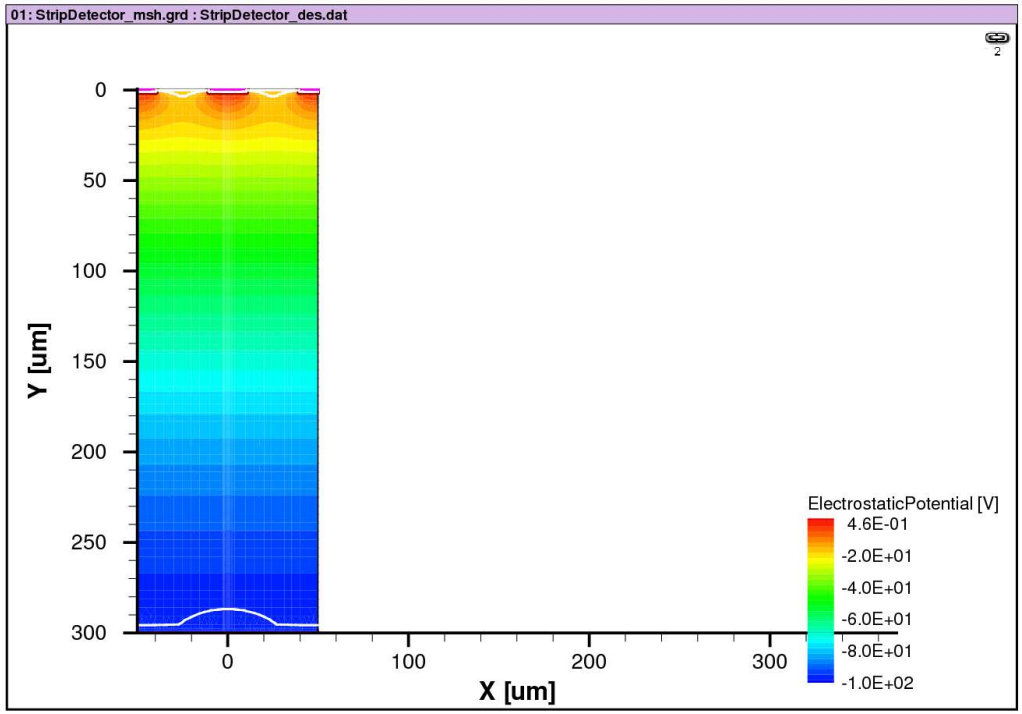

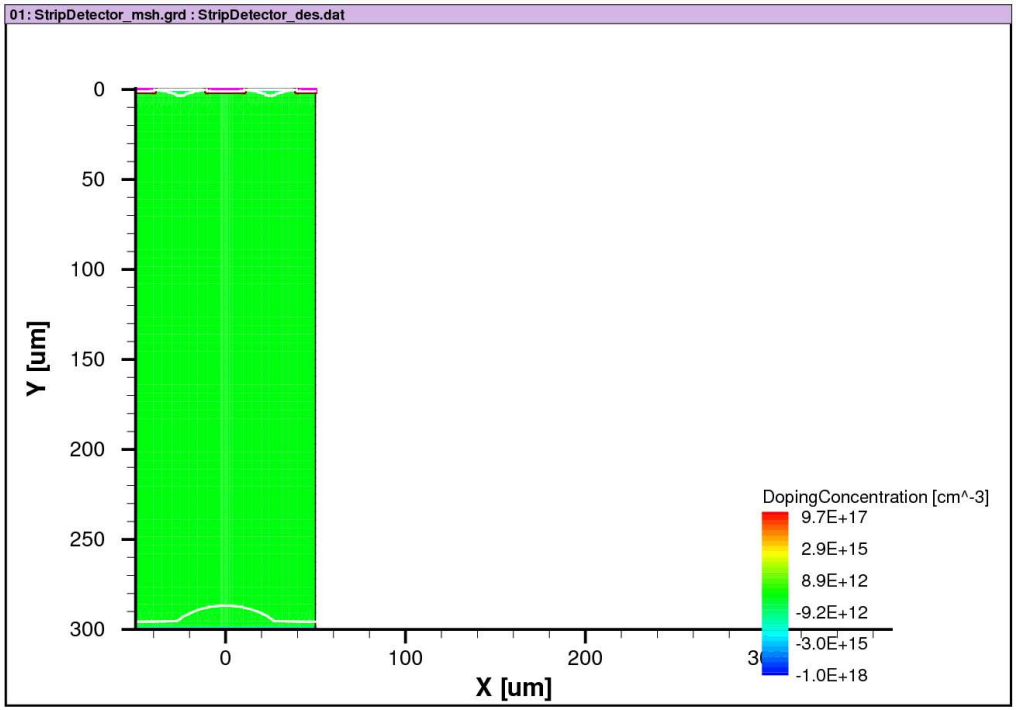

from http://ppewww.physics.gla.ac.uk/det_dev/activities/threedee/Documents/BarcelonaSeminar.html

Boundary element methods

- Contrary to the finite element method, the elements are on the boundaries, not in the problem domain.
- Charges are computed for the boundary elements.

- The fields in the problem domain are calculated as the sum of Maxwell-compliant field functions, not polynomials. There are no discontinuities.

- They do pose numerical challenges due to inherent singularities.

Solution of 3D Poisson's Equation

using BEM

- Numerical implementation of boundary integral equations (BIE) based on Green's function by discretization of boundary.
- Boundary elements endowed with distribution of sources, doublets, dipoles, vortices.

Electrostatics BIE

$$\phi(\vec{r}) = \int_S G(\vec{r}, \vec{r}\,')\rho(\vec{r}\,')\,dS'$$

Potential at r

Charge density at r'

Green's function

$$G(\vec{r}, \vec{r}\,') = \frac{1}{4\pi\epsilon|\vec{r} - \vec{r}\,'|}$$

ε - permittivity of medium

discretization

$$[A]\{\rho\} = \{\phi\}$$

Influence Coefficient Matrix

$$\{\rho\} = [A]^{-1}\{\phi\}$$

Accuracy depends critically on the estimation of [A], in turn, the integration of G, which involves singularities when r → r'.

Most BEM solvers fail here.

Contrast of approaches

nodal versus distributed

Influence of a flat triangular element in Usual BEM

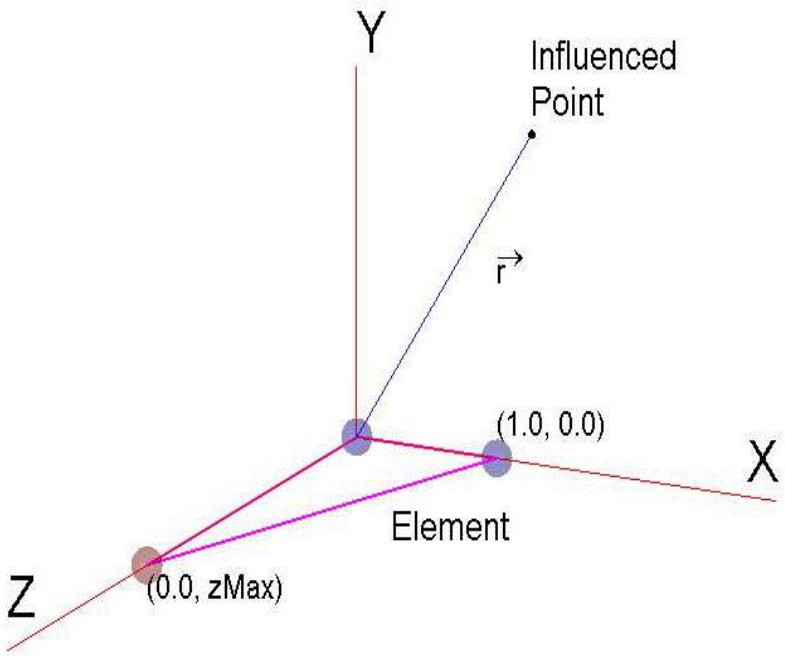

Conventionally, charges are assumed to be concentrated at *nodes*. This is convenient since the preceding integration is avoided. Introduces large errors in the near field.

We have derived exact expressions for the integration of G and its derivative for uniform charge *distributions* over triangular and rectangular elements

Influence of a flat triangular element in ISLES

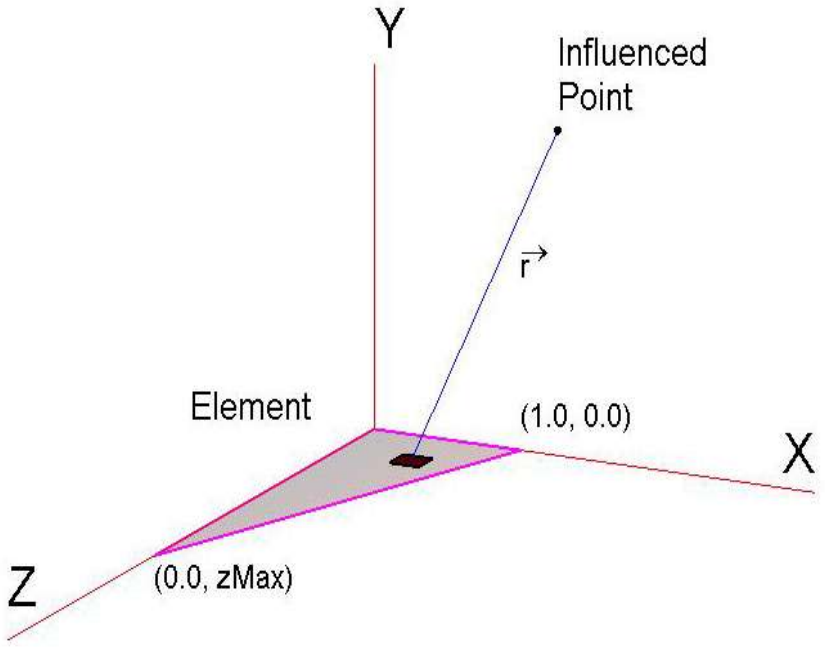

Eletrostatics of Micromegas

FEM Results

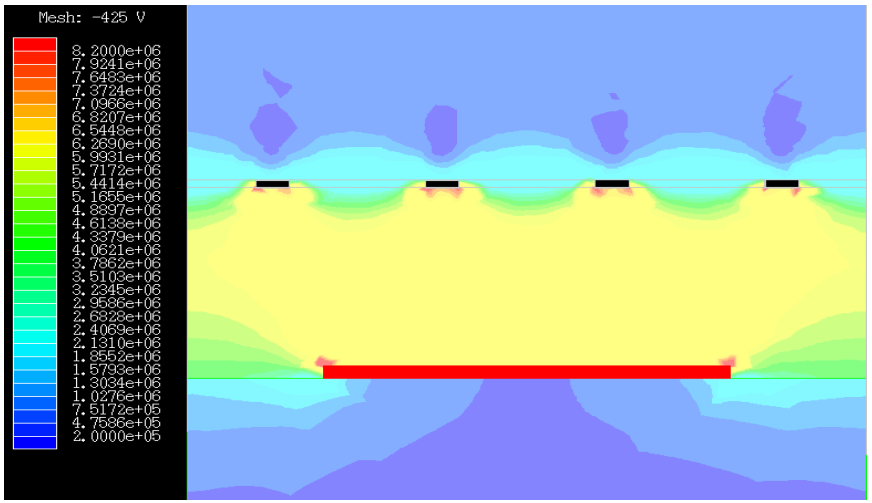

Electric field along hole-centered path line

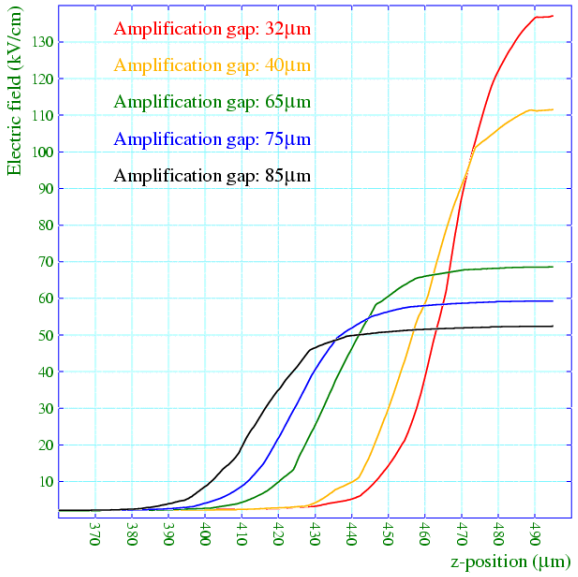

neBEM Results

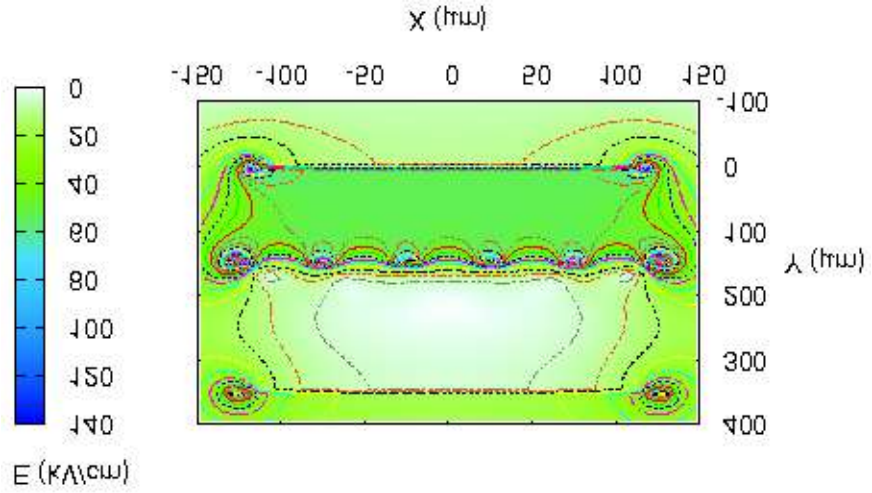

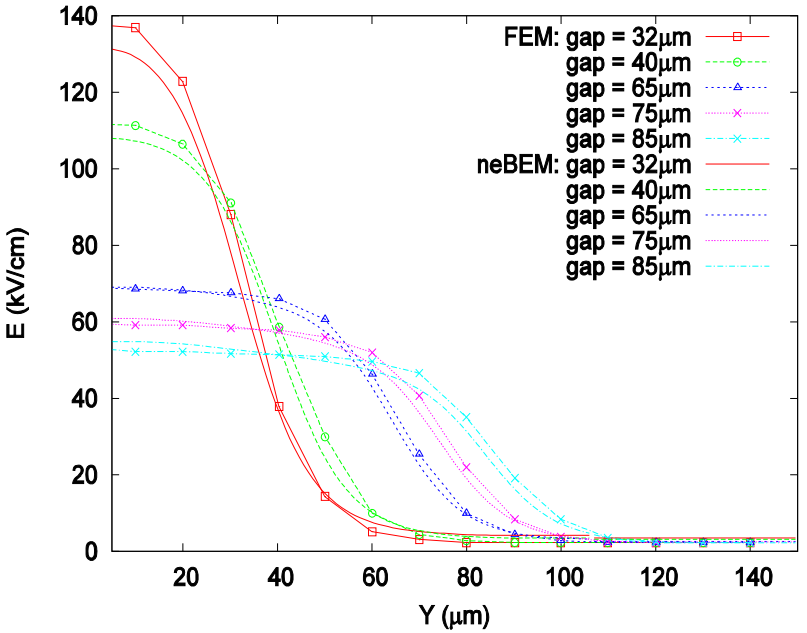

Ar: mean free path

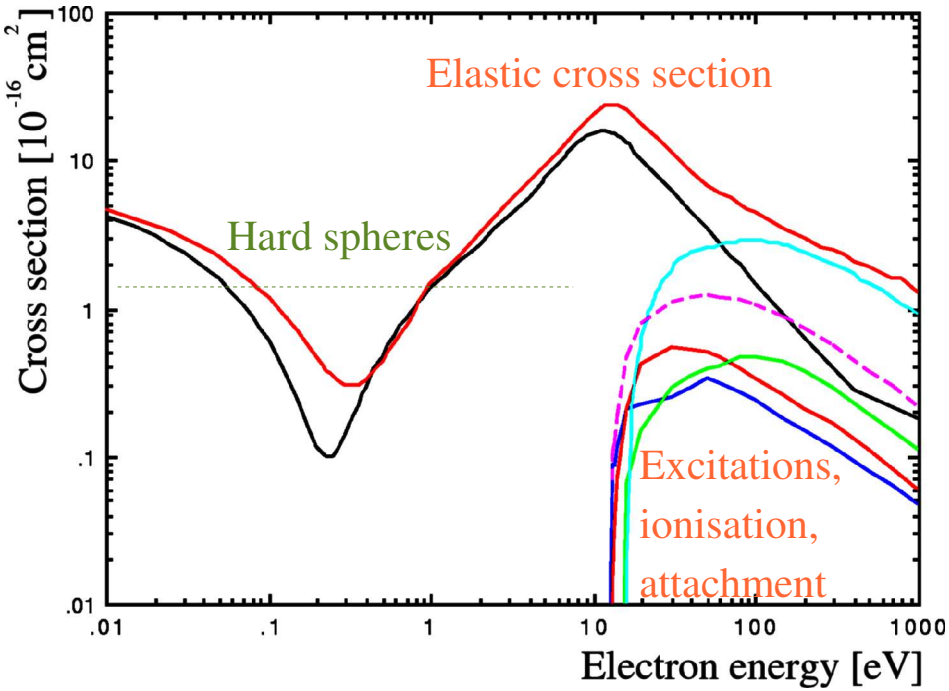

- Using:
  - atomic radius: $r \approx 70$ pm
  - atomic cross section: $\sigma \approx 1.5\ 10^{-16}$ cm^2
  - atoms per volume: $\mathscr{L} \approx 2.7\ 10^{19}$ atoms/cm^3
- Over a distance L, the electron hits $\mathscr{L}\sigma L$ atoms.
- Hence, the mean free path is $\lambda_e = 1/(\mathscr{L}\sigma) \approx 2\ \mu$m.

Scale ≫ mean free path (> 1 mm)

- For practical purposes, electrons from a given starting point reach the same electrode – but with a spread in time and gain.

- Electrons transport is treated by:
  - integrating the equation of motion, using the Runge-Kutta-Fehlberg method, to obtain the path;
  - integrating the diffusion and Townsend coefficients to obtain spread and gain.

- This approach is adequate for TPCs, drift tubes etc.

Runge-Kutta-Fehlberg integration

- Example: a TPC read-out cell

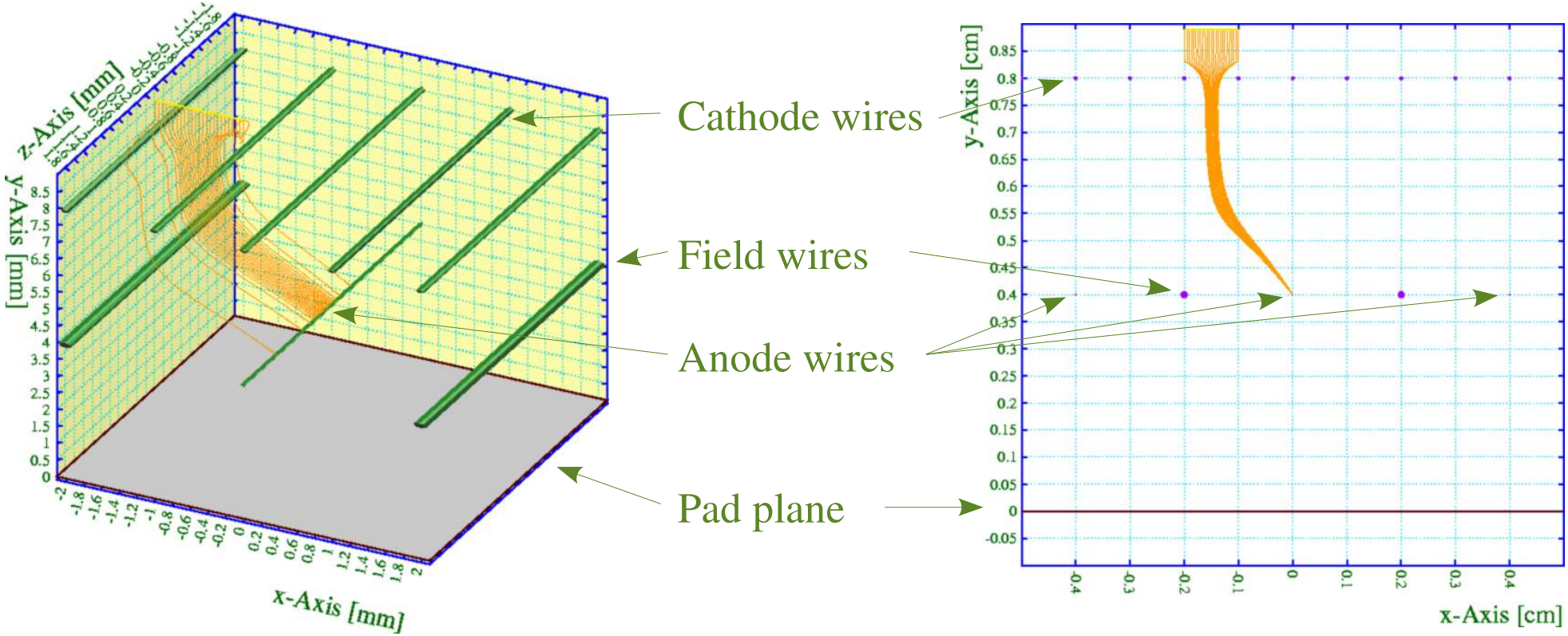

Scale > mean free path (100 μm - 1 mm)

- Electrons from a single starting point may end up on any of several electrodes.
- Calculations use Monte Carlo techniques, based on the mean drift velocity and the diffusion tensor computed by microscopic integration of the equation of motion in a constant field. Gain depends on the path.
- This approach is adequate as long as the drift field is locally constant – a reasonably valid assumption in a Micromegas but less so in a GEM.

Analytic vs Monte Carlo

- Analytic integration
  - Runge-Kutta-Fehlberg technique;
  - automatically adjusted step size;
  - optional integration of diffusion, multiplication and losses.

- Monte Carlo integration
  - non-Gaussian in accelerating, divergent and convergent fields;
  - step size to be set by user.

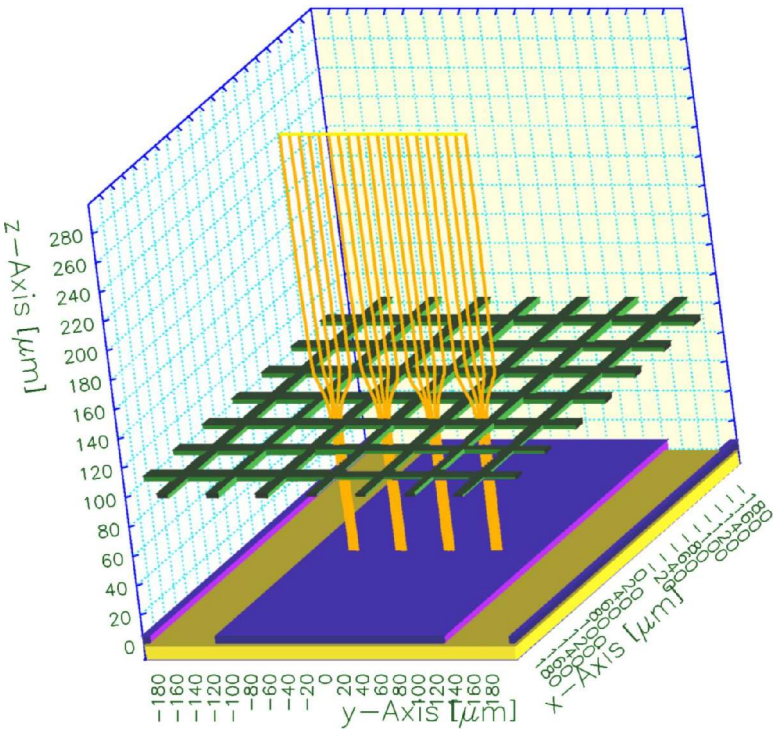

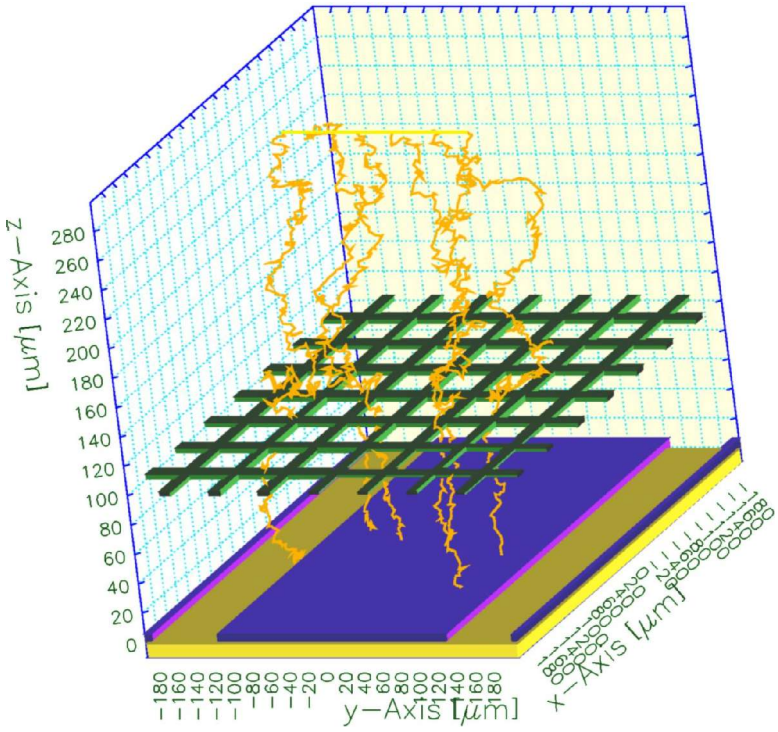

[Figures made by Gilles Barouch, CEA]

Scale ~ mean free path (1-100 μm)

- At this scale, where the mean free path approaches the characteristic dimensions of detector elements, free flight between collisions, is no longer be parabolic.

- The only viable approach here seems to be a complete microscopic simulation of the transport processes, taking local field variations into account.

- The method shown here is based on the Magboltz program.

Molecular tracking: example

- Example:
  - CSC-like structure,
  - Ar 80 % CO_2 20 %,
  - 10 GeV μ.
- The electron is shown every 100 collisions, but has been tracked rigourously.

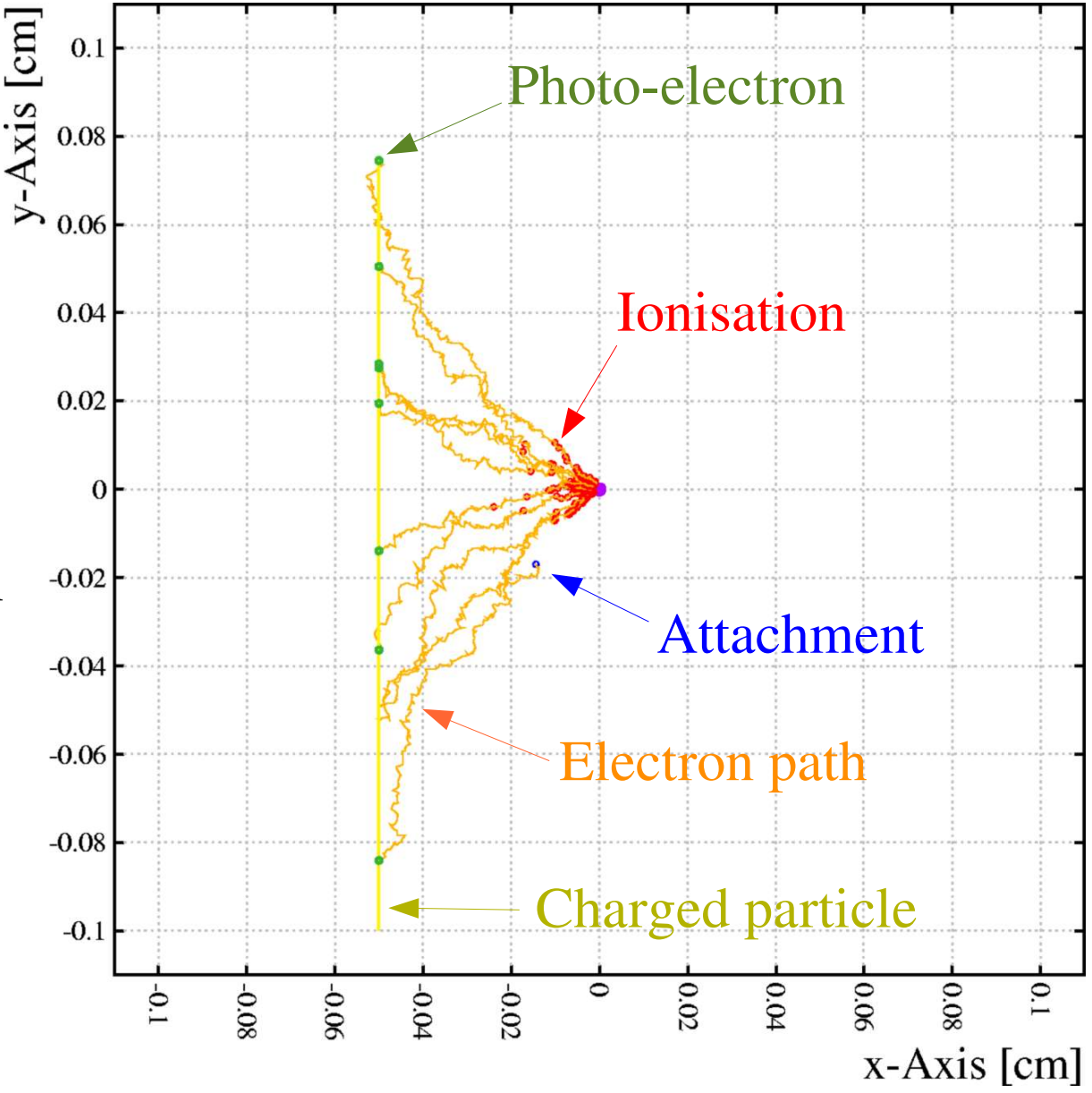

What is in the Magboltz database ?

- A large number of cross sections for 60 molecules...
  - All noble gases, *e.g.* argon:
    - elastic scattering,
    - 3 excited states and
    - ionisation.
  - Numerous organic gases, additives, *e.g.* CO_2:
    - elastic scattering,
    - 44 inelastic cross sections (vibrations, rotations, polyads)
    - 35 super-elastic cross sections,
    - 6 excited states,
    - attachment and
    - ionisation.

Argon

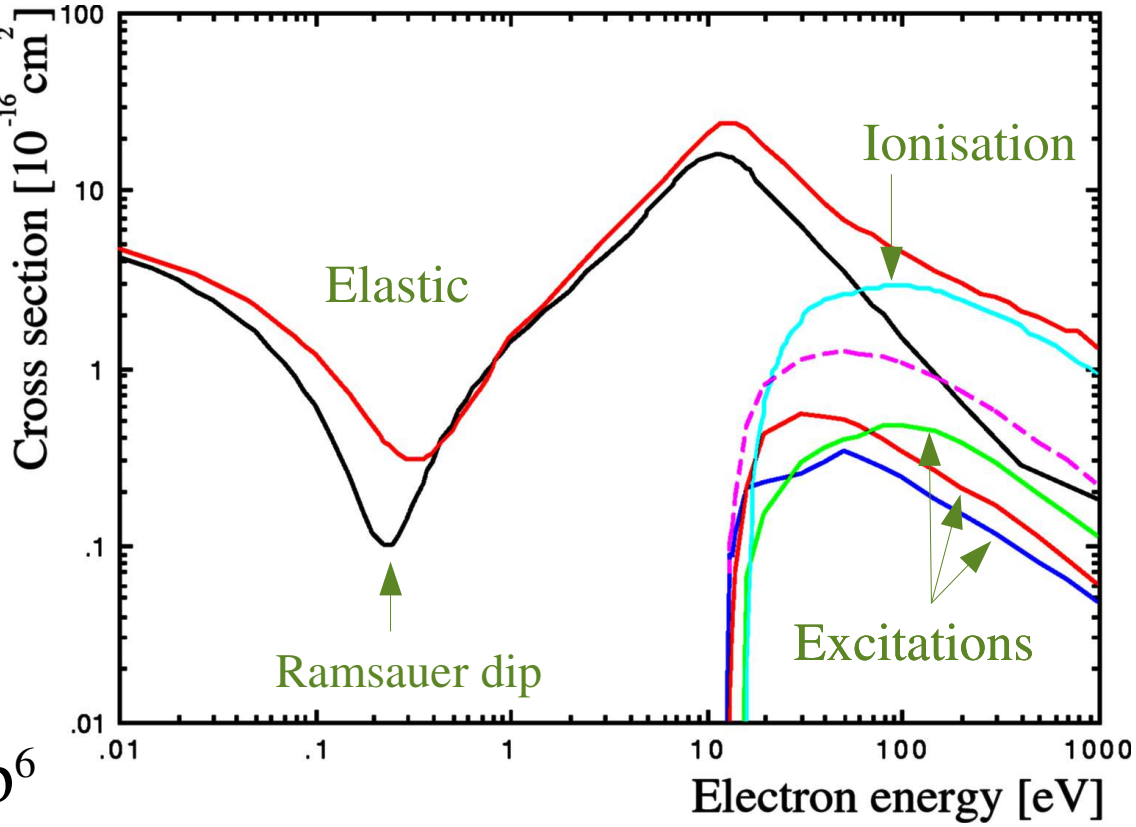

- Elastic scattering:
  - dominant till ~50 eV;
  - features Ramsauer dip
- Ground state: [Ne] $3s^2\,3p^6$

  the lowest excited states have an e^- in the
  - 3rd shell: [Ne] $3s^2\,3p^5\,3d^1$, or
  - 4th shell: [Ne] $3s^2\,3p^5\,4s^1$, [Ne] $3s^2\,3p^5\,4p^1$, ...
- Attachment is not significant.
- Ionisation
  - occurs from 15.7 eV;
  - 2 levels: $3p^5$ spin and orbital angular momentum ↑↑ or ↑↓.

Argon levels

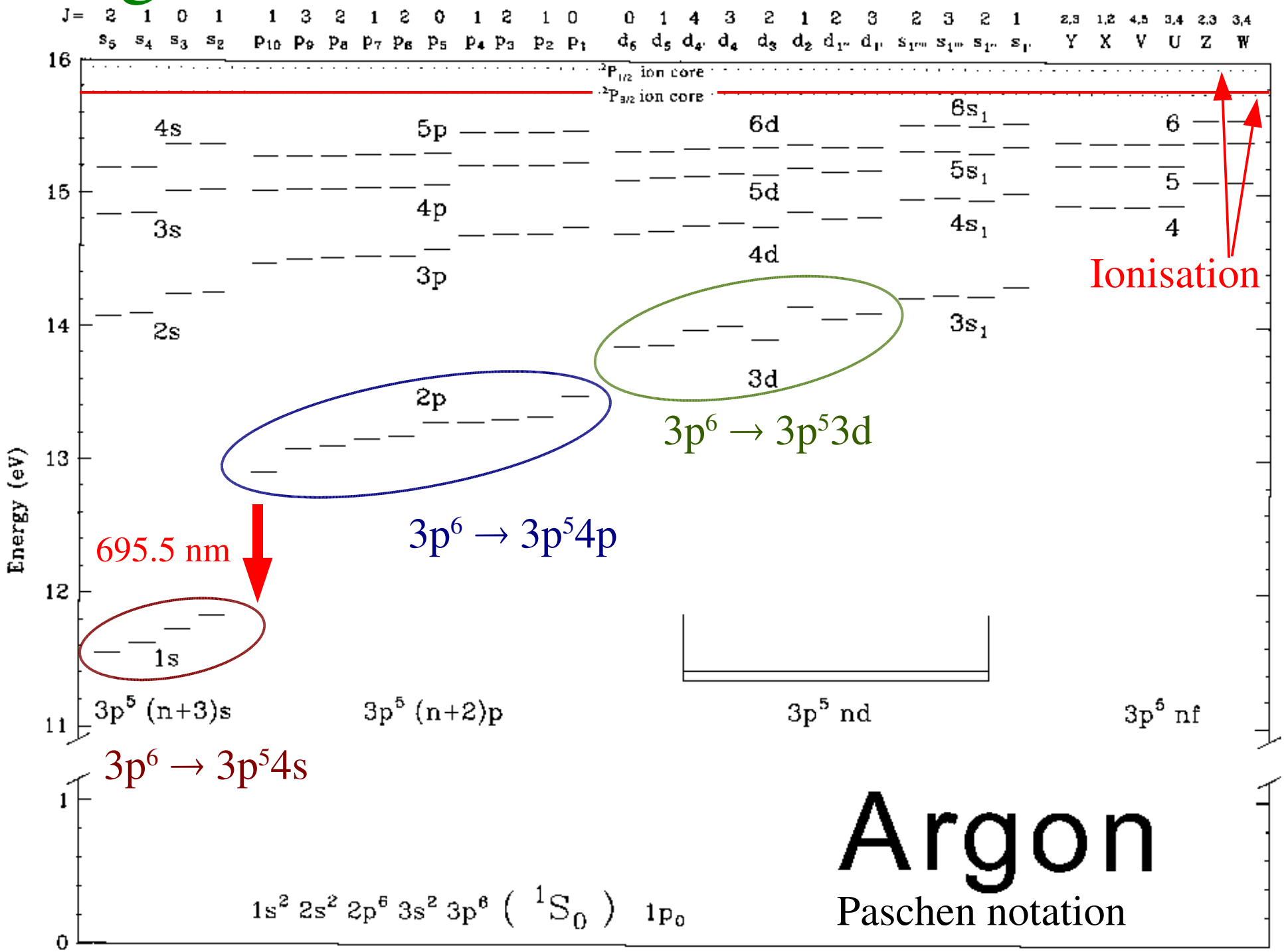

CO_2 – vibration modes

- CO_2 is linear:
  - O – C – O
- Vibration modes are numbered V(*ijk*)
  - *i*: symmetric,
  - *j*: bending,
  - *k*: anti-symmetric.

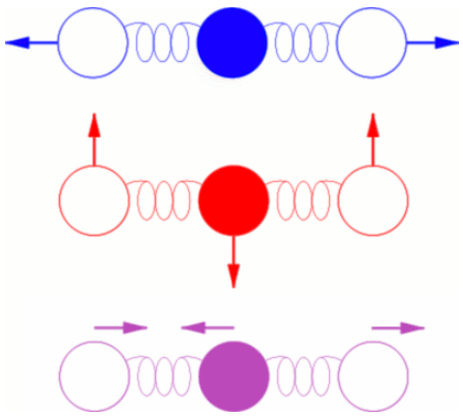

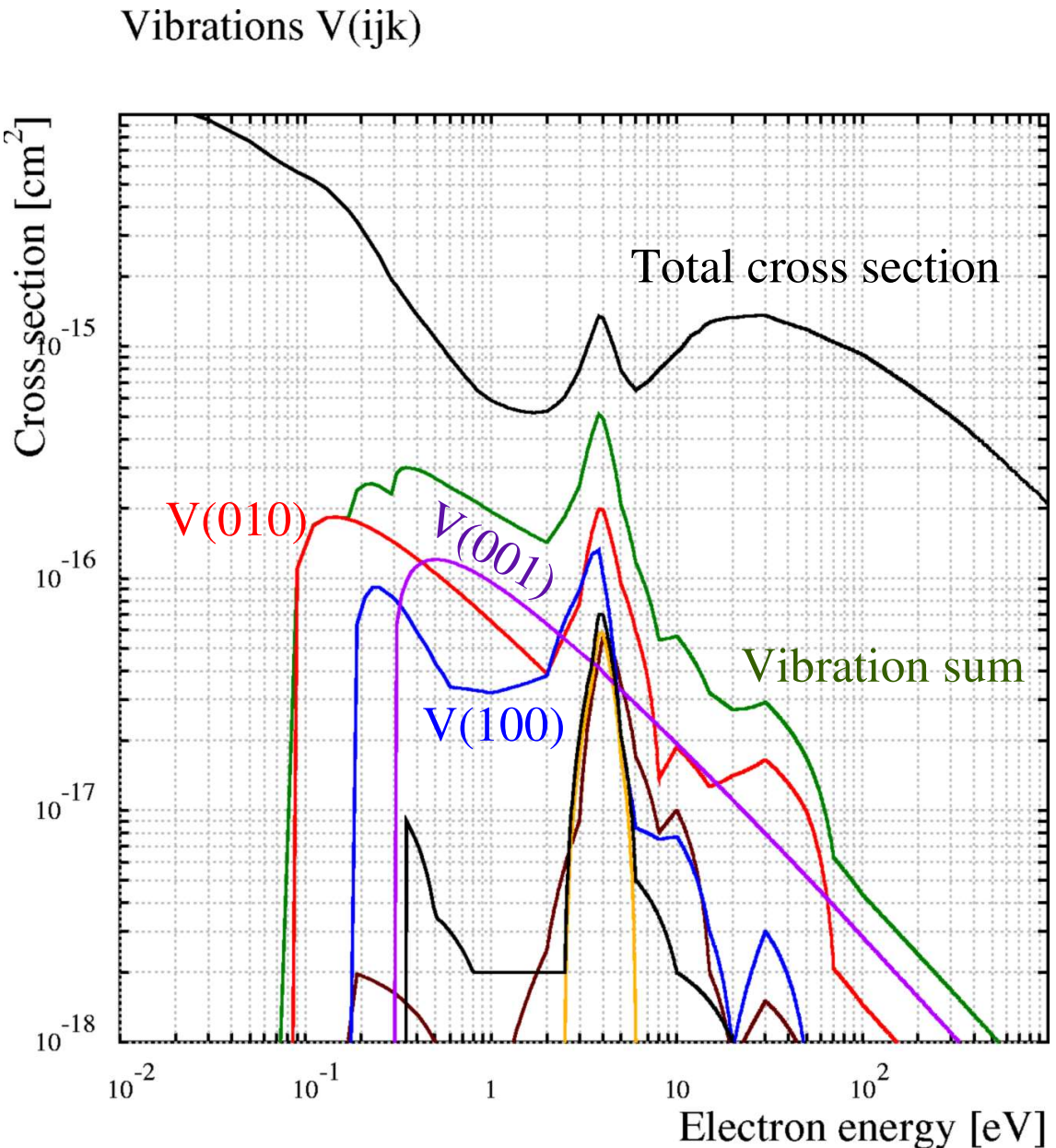

Verification: drift velocity Ar/CO_2

- In a constant field, Magboltz and the molecular tracking procedure should give identical results.
- This is shown to hold for the Ar CO_2 mixture.

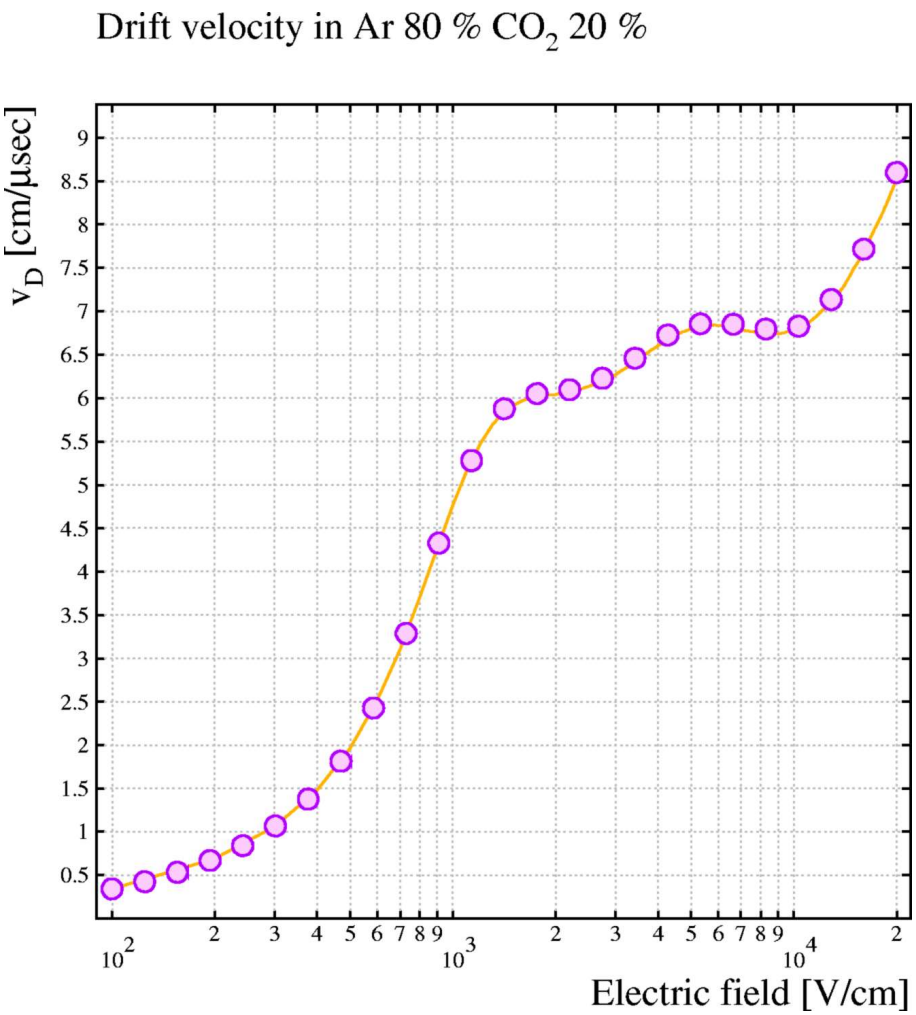

Diffusion in Ar/CO_2

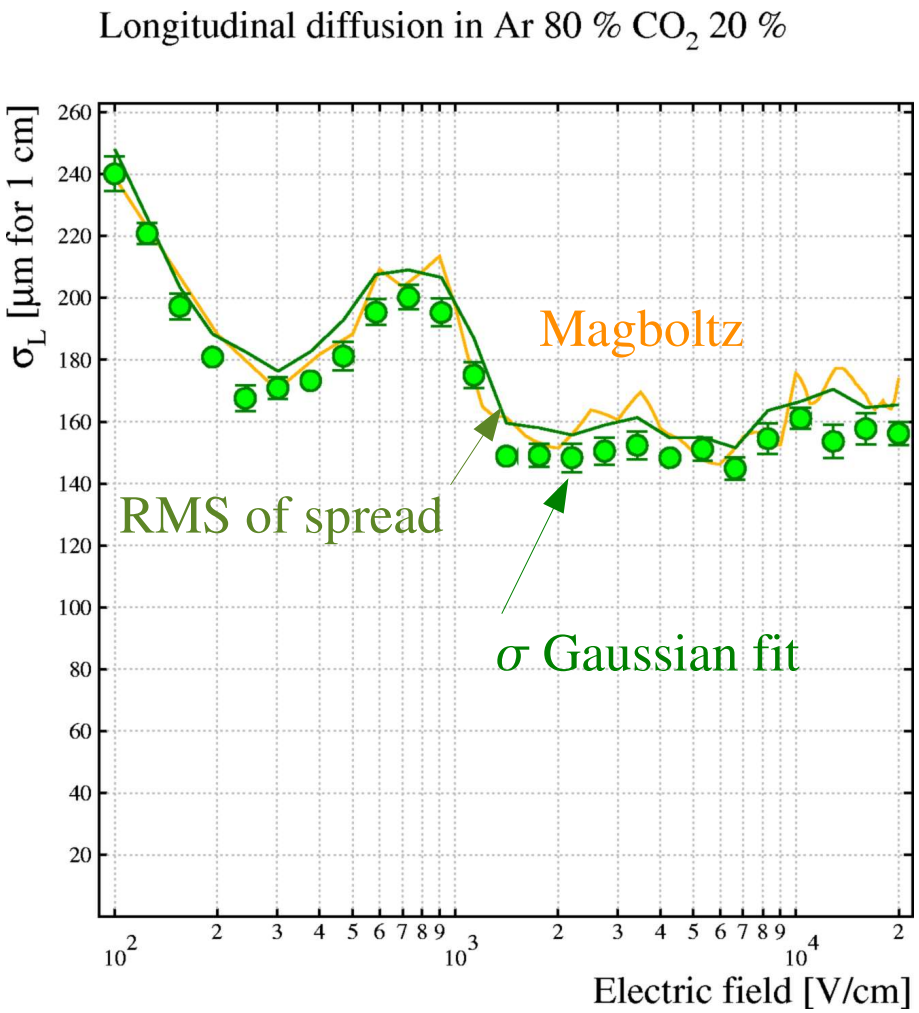

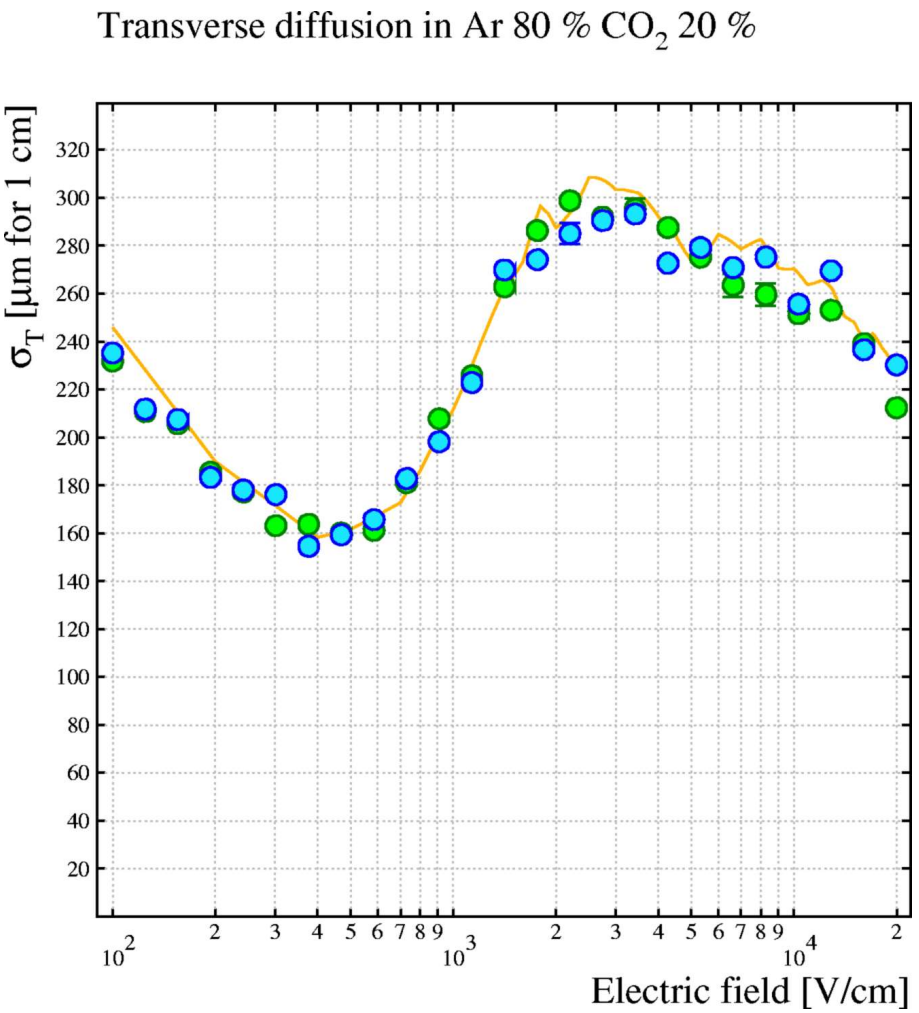

Multiplication in Ar/CO_2

- In a constant, low field there is agreement.
- More on higher fields ...

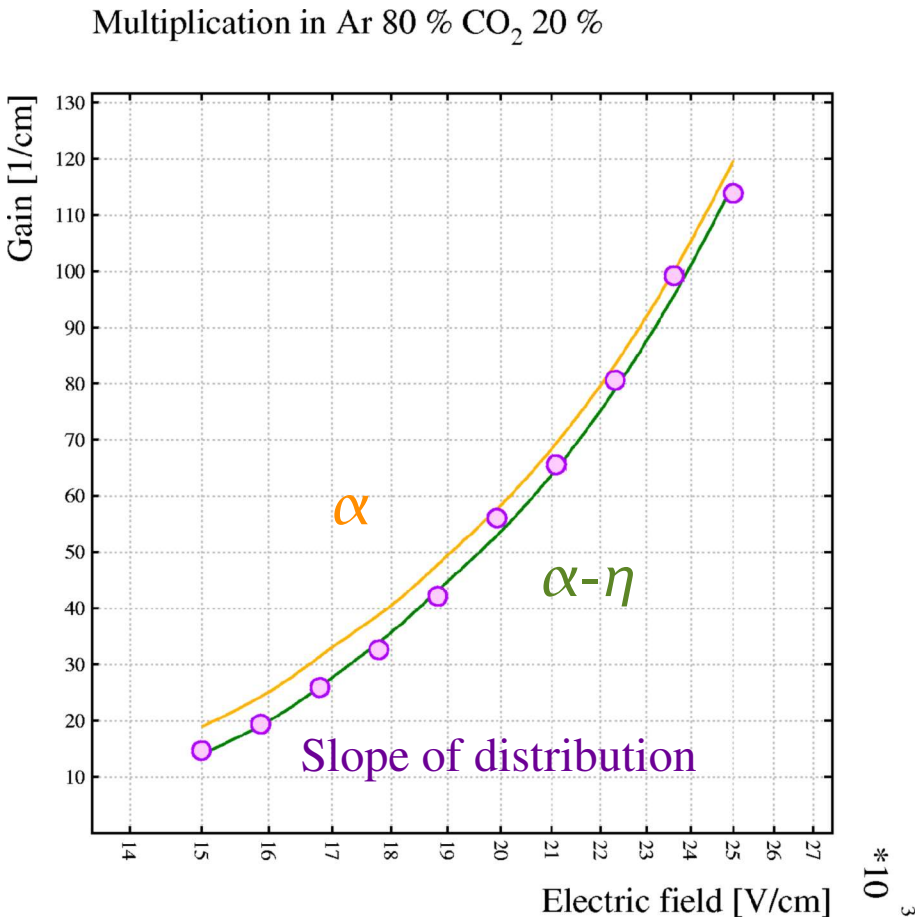

Ar/CO_2: size distribution

- With increasing field, the size distribution becomes more and more "round":

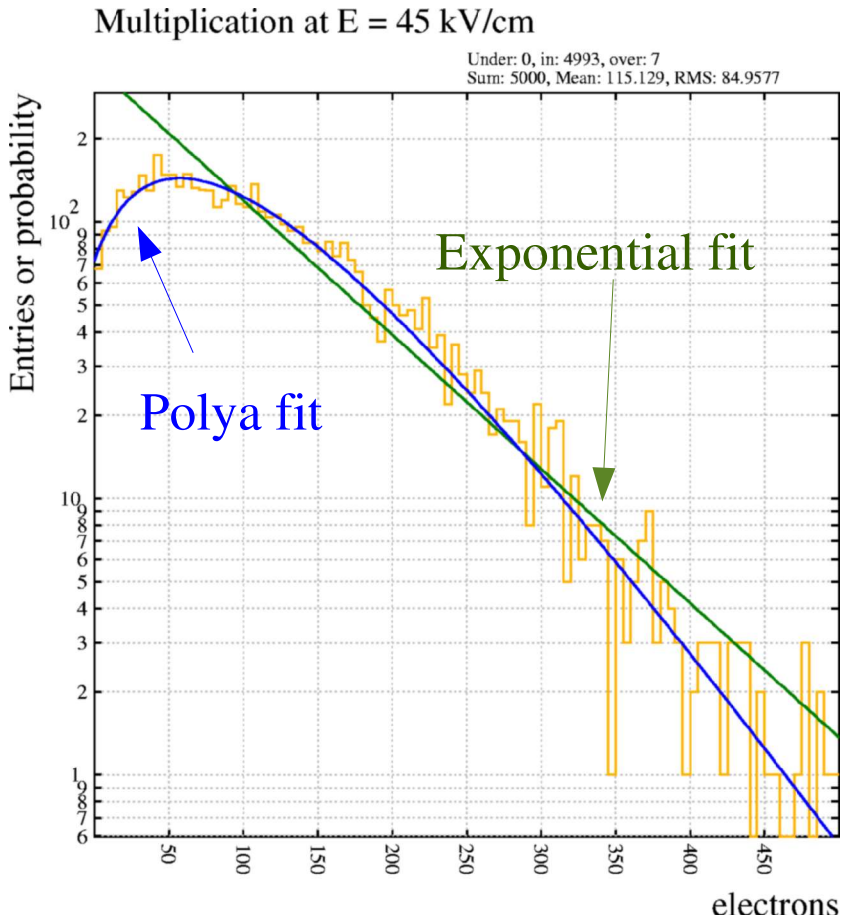

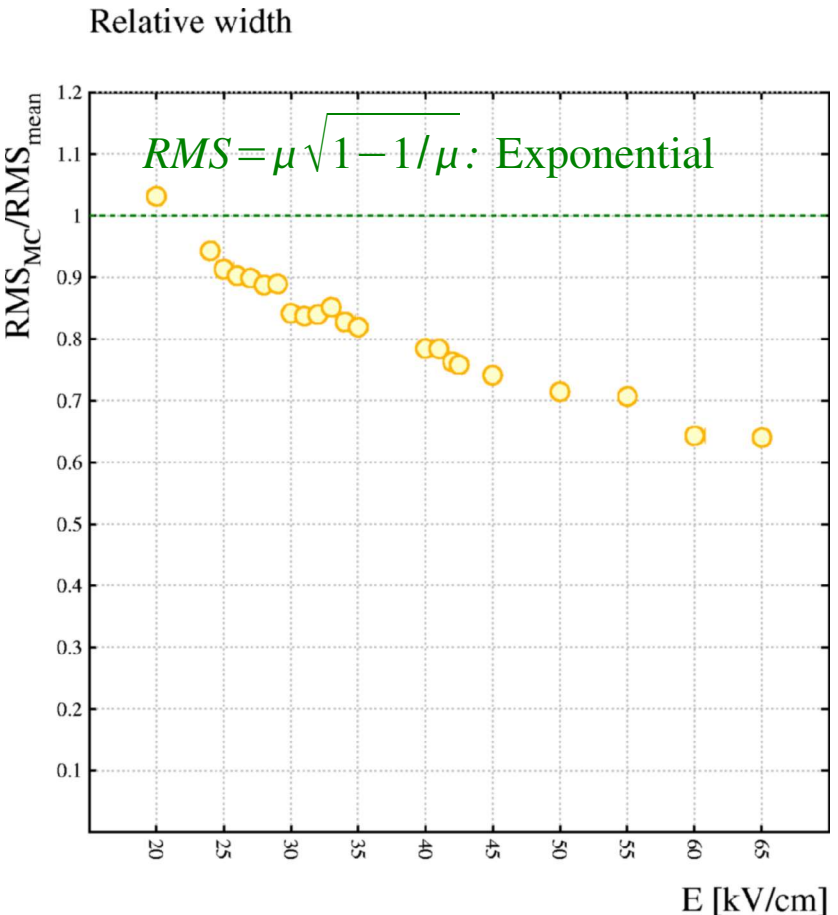

Summary

- Inspite of the long history of gas-based detectors, understanding of their behaviour still improves.
- Calculations for gas detectors are therefore steadily becoming more detailed, and it becomes more and more important for the users to understand the model.
- In some domains, *e.g.* signal shapes, one can easily verify the calculations by hand. In others, *e.g.* the gas properties, this is unfortunately far from trivial.